

CASE FILE
COPY

NATIONAL ADVISORY COMMITTEE
FOR AERONAUTICS

TECHNICAL MEMORANDUM

No. 1107

SIX-COMPONENT MEASUREMENTS ON A STRAIGHT AND A
35° SWEPT-BACK TRAPEZOIDAL WING WITH AND
WITHOUT SPLIT FLAP

By G. Thiel and F. Weissinger

Translation

“Sechskomponentenmessungen an einem geraden und einem
35° rückgefeilten Trapezflügel ohne
und mit Spreizklappe”

Deutsche Luftfahrtforschung, Untersuchungen und Mitteilungen No. 1278



Washington

June 1947

NATIONAL ADVISORY COMMITTEE FOR AERONAUTICS

TECHNICAL MEMORANDUM NO. 1107

SIX-COMPONENT MEASUREMENTS ON A STRAIGHT AND A
35° SWEEP-BACK TRAPEZOIDAL WING WITH AND
WITHOUT SPLIT FLAP*

By G. Thiel and F. Weissinger

SUMMARY

The six-component measurements on a straight and a
35° swept-back trapezoidal wing $\left(\frac{b^2}{F} = 5; \frac{l_i}{l_a} = 2; \right.$

NACA airfoil section 0012; normal rounding of tips),
which differ from each other only in sweepback, have
indicated the following results:

A. Unstalled Flow Regime

Without flaps the rolling moment due to yaw of both
wings (for $\beta > 0$) is positive, the leading wing is
raised, the yawing moment due to yaw negative (restoring).
A comparison of the straight trapezoidal wing with the
corresponding straight rectangular wing indicates that
the magnitude of the moments is reduced by the taper, as
stipulated by theory; the agreement is also good quanti-
tatively. The magnitude of the rolling moments due
to yaw and of the yawing moments due to yaw is substan-
tially increased by the sweepback; this effect is likewise
reproduced satisfactorily by the theory.

Even with flaps the rolling moments due to yaw and
the yawing moments due to yaw are greater on the wing with

*"Sechskomponentenmessungen an einem geraden und
einem 35° rückgefeilten Trapezflügel ohne und mit
Spreizklappe." Zentrale für wissenschaftliches Bericht-
swesen der Luftfahrtforschung des Generalluftzeugmeisters
(ZWB), Untersuchungen und Mitteilungen No. 1278.
Aug. 1, 1944.

sweepback than on that without it. On the straight wing a flap deflection has the effect of a variation in profile camber: at $c_a = 0$ a negative rolling moment due to yaw exists, while the increase with c_a is about the same as without flaps. On the swept-back wing also the increase of the rolling moment due to yaw with c_a is not essentially modified by flap deflection, but the moment is considerably dependent on the flap width at $c_a = 0$; with 50 percent flaps the swept-back wing has the same (negative) zero-lift moment as the straight wing, while for the full span (100 percent) flaps a zero-lift moment of about twice the moment and opposite (positive) prefix was recorded. This ties in with the observation that the lift of the straight wing with flaps in yaw remains zero under constant angle of attack, when it disappears for $\beta = 0$, while the swept-back wing in this instance receives positive lift. These phenomena, which rest on the fact that on the swept-back wing the adjustment of the angle of attack is not accomplished by rotation about the $l/4$ line as on the straight wing, can be explained theoretically; the agreement with the test data is good.

B. Behavior At Maximum Lift

Except for too small Reynolds numbers the maximum lift, especially the effect of flap deflections, is reduced by sweepback, as proved by the present measurements. However, the effect is known to be greatly dependent on the Reynolds number, so that the secured data cannot be arbitrarily generalized. Noteworthy - in contrast to other swept-back airfoil measurements at similar R_e - is a comparatively high $c_{a_{max}}$ increase owing to flap deflection.

The breakdown of flow on the swept-back wing is characterized by great sudden variations in the rolling moments due to yaw with minor lift changes as well as by tail heavy (stalling) acting variations of the pitching moment, while the rolling-moment variations of the straight wing are somewhat smaller and associated with great lift changes and nose-heavy pitching-moment variations. The cause of this dissimilar behavior is that the flow on the straight wing breaks down first in the central part of the span, on the swept-back wing first at the tips.

I. INTRODUCTION

In accord with the test program (published in reference 7) the wing in question is briefly designated as No. 5. It differs from the rectangular wing (No. 1) discussed in reference 7 by its taper and from the 35° swept-back trapezoidal wing (No. 9) treated in reference 8 by the absence of sweepback.

Since the effect of sweepback can be investigated only in the light of the data on the straight wing an interpretation of the test data on the swept-back wing was omitted in (8). The present report consists therefore of two principal parts: section V deals above all, respectively, with the straight trapezoidal wing (No. 5) and by having recourse to the rectangular wing (No. 1) with the effect of taper, while section VI is primarily concerned with the swept-back wing (No. 9), and with wing No. 5 merely as comparative wing.¹

II. NOTATION

Lift, drag and transverse force are referred to the wind axis system (DIN L 100), the pitching, rolling, and yawing moments to the experimental system of axes (cf. reference 5). The origin the coordinate systems is placed on the profile chord of the central section at 1/4 wing chord. While the pitching moment of the swept-back wing (No. 9) is, as in reference 8, referred to the measured quarter-chord point of the smooth wing (no landing aids), the lateral axis placed at quarter-chord point which is little behind the measured neutral point, was chosen as reference axis, as for wing No. 1. For the rest of the definitions see figure 1.

V airspeed

ρ air density

¹According to oral report from the Junkers Co. comprehensive test data on swept-back wings (especially also with flap deflections) are available but have never been made public.

$q = \frac{\rho}{2}V^2$	dynamic pressure
F	wing area
b	span
l	wing chord
l_i	wing chord inside (wing center)
l_a	wing chord outside (wing tip)
$l_m = \frac{F}{b}$	mean wing chord
$\Lambda = \frac{b^2}{F}$	aspect ratio
$Z = \frac{l_i}{l_a}$	taper
ϕ	angle of sweepback (referred to $l/4$ line, positive for swept-back wing)
Re	Reynolds number
α_k	geometric angle of attack with respect to tunnel axis
α	angle of attack corrected for slipstream inclination, tunnel-wall interference effect and wire length
β	angle of slip
$A = c_a q F$	lift
$W = c_w q F$	drag (in air-stream direction)
$Q = c_q q F$	transverse force (perpendicular to air- stream direction)
$Y = c_y q F$	lateral force (spanwise direction)

$M = c_m q F l_m$ pitching moment

$M_n = c_{Mn} q F l_m$ pitching moment (referred to neutral point
of smooth wing)

$L = c_L q F \frac{b}{2}$ rolling moment

$N = c_N q F \frac{b}{2}$ yawing moment

$c_a' = \frac{dc_a}{da}$ lift increment

$c_a'_{\infty}$ profile constant $\left(\frac{dc_a}{da} \text{ at } \Lambda = \infty \right)$

The subscript 0 indicates that the respective coefficient is to be taken at equal β for $c_a = 0$.

The subscript g signifies that the coefficient refers to equal a at $\beta = 0$ (g = straight air flow), subscript Pf that only the sweepback effect (the difference between the wing with and without sweepback) is considered.

III. DESCRIPTION OF MODEL

Wing No. 5 was manufactured of reinforced plywood, its dimensions are given in figure 2. The $l/4$ line is straight, the taper Z amounts to 2. Without end cap the wing span is 1.5 m and the mean chord 0.3 m, hence the aspect ratio $\Lambda = 5$. On account of the "normal" rounding of the tips (semicircular with the local half profile thickness as radius) with which the wing is fitted, wing area, span, and aspect ratio are increased by 0.7 percent, 1.6 percent and 2.5 percent; however, the coefficients in the following are always referred to the mass of non-rounded wing ($F = 0.45 \text{ m}^2$; $b = 1.5$). Apart from the end cap the wing has the NACA section 0012 along the span; dihedral and warping are absent.

The split flaps, which extend 100 percent and 50 percent (inside) across the span, were attached at

80 percent wing chord and formed a 60° angle with the profile tangent (fig. 2).

IV.- TESTING PROCEDURE AND INTERPRETATION OF TESTS

The tests were run in the medium wind tunnel of the DVL at $q = 156 \text{ kg/m}^2$ ($Re \approx 1 \times 10^6$) dynamic pressure. The six-component measurements were run over the angle of yaw, that is, angle β was varied at 5° each between 30° and -30° with fixed angle of attack α_K . For $\beta = \pm 20^\circ$ (and naturally for $\beta = 0$) the angle of attack was varied for fixed β . Because of the symmetry control the measurements were always made for positive and negative β , and also for several negative c_a values on the wing without and with 50 percent split flaps. The symmetry was satisfying, though not quite as good as on wing No. 9, which being of all metal, could be manufactured particularly accurate. The asymmetry of the drag with respect to α , already observed on wing No. 9, was noted again.

The suspension system is illustrated in figure 3. To avoid a disturbance of the transverse force, no moment lever was used, the wire leading to the moment balance was attached to a small eye located directly behind the wing trailing edge and also carried part of the initial load. The rest of the initial load being on a wire which applied on the straight line connecting the two forward bearings. This wire forms the sole disturbance of the suction side, so that it can be regarded as practically undisturbed. Care was again taken to prevent any air from passing from the pressure side to the suction side. The wires were of round section.

The angle of attack α is corrected for tunnel-wall interference effect. The wire length, however, was then not taken into consideration, since its effect on α was very small according to several sampling tests. The corrections on the forces and moments followed the customary procedure, with due consideration to the relationship existing between angle of attack α_K and pitching-moment correction.

In the charts with respect to α (figs. 7 to 9) a correction of the symmetry with respect to β was omitted

as in reference 8, while in those with respect to β the test values averaged for $\pm\beta$ are represented. The derivations with respect to β were formed by dividing the test values averaged for $\beta = 5^\circ$ by $5 \times \frac{\pi}{180}$.

V. RESULTS OF TESTS ON STRAIGHT WING,

COMPARISON WITH THEORY

A. Straight Air Flow

1. Without flaps (figs. 4 and 7).- Conspicuous on the curves $c_a(\alpha)$, $c_w(\alpha)$, $c_M(\alpha)$ is the marked depression in the c_M -curve, which as on the rectangular wing (reference 7, fig. 7) sets in at about $\alpha = 6^\circ$ and is at the same time associated with a temporary rise in $\frac{dc_a}{d\alpha}$. The curve of $c_a(\alpha)$ for wing No. 5 and wing No. 1 is, up to the $c_{a_{max}}$ of the latter, almost identical (theoretically the $\frac{dc_a}{d\alpha}$ of wing No. 5 should be about 2 percent greater), the c_{max} of wing No. 1 is about 2° , the $c_{a_{max}}$ about 0.03 smaller than for wing No. 5. The polar $c_a(c_w)$ of both wings agrees up to $c_{a_{max}}$, while theoretically the induced drag of wing No. 1 should be about 4 percent higher than that of wing No. 5.

2. 100-percent flaps (figs. 6 and 9).- With split flaps over the entire span the maximum lift coefficient for wing No. 5 is 0.2 higher than for wing No. 1 (cf. reference 7, fig. 9). Unusual and not quite explainable is the dissimilarity in zero lift angle - 12.8° for wing No. 5 and -12° for wing No. 1. This as well as the (slight) curvature of $c_a(\alpha)$ and the substantial curvature of $c_M(\alpha)$ near $c_a = 0$ is perhaps attributable to separation phenomena. As for the rest, the difference in the c_M of both wings is due in part to the fact that the coefficient was formed with the reference chord $l_m = \frac{F}{b}$ rather than with the so-called aerodynamic wing chord. The conversion of the $c_{M0} \approx 0.203$ value of wing No. 1 to No. 5 would give $c_{M0} = -0.211$, as against $c_{M0} = -0.228$ by measurement. The polar of wing

No. 1 is shifted toward the right by the constant amount $\Delta c_w \approx 0.28$, for which also no true reason can be seen.

3. 50-percent flaps (figs. 5 and 8).- With flaps over 50 percent of the span the $c_{a_{max}}$ of wing No. 1 is 0.1 smaller than that of wing No. 5. The zero lift angles are -8.3 percent for wing No. 5 and -7.3° for wing No. 1. Utilizing the profile characteristic $\alpha_0 = -12^\circ$ gives, theoretically, $\alpha_0 = -7.25^\circ$ for wing No. 5 and $\alpha_0 = -6.76^\circ$ for wing No. 1. That the measured difference exceeds 0.5° is probably due to the deviation with full-span flaps. The reduction of the moment $c_{M_0} \approx -0.103$ measured on the rectangular wing to the trapezoidal wing gives $c_{M_0} = 0.141$ instead of the measured $c_{M_0} \approx -0.145$. The induced drag of the rectangular wing is less than that of the trapezoidal wing.

B. YAWED FLOW

A correlation of the test data for the area of sound flow² is to be found in the figures 13 to 16, while the adjoining figures indicate further interpretations of these results. Regarding the various coefficients the following should be noted:

1. Lift.- Dividing the lift existing for angle of yaw β by the lift at $\beta = 0$ and equal angle of attack should give, theoretically, $\cos^2\beta$. This law is very rigorously complied with, for both with and without flaps, according to figure 21³.

2. Drag.- The drag of the wing without flaps diverges in part considerably from the $\cos^2\beta$ law (cf. fig. 21). This departure might in a large measure be attributable to the instrumental inaccuracy caused by the smallness

²At the highest angles of attack shown, breakdown phenomena are already visible in part.

³In figures 21 and 22 points which actually should merge are pulled apart along the β -axis, that is, placed along side each other.

of c_w and in part to the friction drag which certainly need not behave like $\cos^2\beta$. With 100 percent flaps the test points c_w/c_{wg} lie better on the curve $\cos^2\beta$, while in this instance, wing No. 1 rather followed a $\cos^3\beta$ law.

At zero lift the drag of the wing with continuous split flaps consists practically only of pressure drag introduced by the dead-air region of the flaps; the resulting force is therefore parallel to the plane of symmetry of the wing in yawing. Since the effective air-speed in yawing becomes smaller by the factor $\cos\beta$, the pressure drag varies by the factor $\cos^2\beta$ and hence the drag coefficient $(c_w)_{c_a=0}$ (parallel to wind direction) by the factor $\cos^3\beta$. Why the wing No. 5 in contrast to wing No. 1 does not follow this law is not evident. Theoretically, the induced drag must, as explained in reference 7 act as $\cos^2\beta$.

3. Pitching moment.- For the pitching moment with and without flaps the $\cos^2\beta$ law also agrees very well (cf. fig. 23), that is, the neutral point and the center of pressure position are not affected by yawing. At high c_a values the variation with flaps is a little less than $\cos^2\beta$.

4. Transverse force, cross-wind force.- With the coefficients of pressure, friction, and induced drag denoted by c_{wD} , c_{wR} , and c_{wi} (where c_{wD} and c_{wi} signify forces perpendicular to the $l/4$ line, while c_{wR} is parallel to the wind),

$$c_w = \cos\beta (c_{wD} + c_{wi}) + c_{wR} \quad (1)$$

$$c_q = -\sin\beta (c_{wD} + c_{wi}) = -\text{tg}\beta (c_w - c_{wR}) \quad (2)$$

$$c_y = \sin\beta \times c_{wR} \quad (3)$$

therefore

$$\frac{\partial c_q}{\partial \beta} = - (c_{wg} - c_{wRg}) \quad (4)$$

$$\frac{\partial c_y}{\partial \beta} = c_{wR} g \quad (5)$$

For the friction drag c_{wR} without flaps the profile drag c_{wp} may be used. Nothing is known about the friction drag with flaps, so for the want of something better the value c_{wp} without flaps will be used.

Without flaps formula (4) agrees completely, as seen in figure 17. The agreement is also satisfactory with flaps; it would become better even in this case after striking of the friction term.

The cross-wind force is not measured directly by the balance of the medium wind tunnel, but computed from the transverse force and the drag. Since these are not very accurately measured and largely carried out for the composition of the cross-wind force, the determination of the cross-wind force is not very reliable as evinced by the marked scatter and the inferior systematic curve distribution of figures 16 and 18. Moreover, negative values of $\frac{\partial c_y}{\partial \beta}$, as they occur on the wing with flaps, seem quite improbable. In view of this instrumental inaccuracy and the smallness of $\frac{\partial c_y}{\partial \beta}$ no agreement with theory is of course to be expected. At any rate formula (5) without flaps agrees at least in order of magnitude.

5. Rolling moment.-- In figure 19 the derivation $\frac{\partial c_L}{\partial \beta}$ of the rolling moment due to yaw is plotted against the lift coefficient. By theory (reference 11)

$$\frac{\partial c_L}{\partial \beta} \cong \frac{\partial c_{L0}}{\partial \beta} + \left[\frac{2x}{\Lambda} \frac{1 + 0.15 (Z - 1)}{Z + 1} - 0.10 \right] C_{ag} \quad (6)$$

For wing No. 5 without flaps $\frac{\partial c_{L0}}{\partial \beta}$ should really be zero by reason of the symmetrical profile; that the measured

curve does not go exactly through the zero point is likely to be due to design or jet inaccuracies. For the empirical factor x , the value $x = 1.2$ is optimum (cf. reference 1 and 11) and figure 19 actually shows the theoretical curve with $x = 1.2$ to be coincident with the measured curve to a large extent. A flap deflection should act like a profile camber on the rolling moment due to yaw, that is (reference 3 and 12) it should

$$\frac{\partial c_{L0}}{\partial \beta} = \frac{2}{\Lambda} c_{M0} \quad (7)$$

where c_{M0} is the measured zero lift moment of the whole wing. With the previously employed c_{M0} values we get, for 50-percent flaps, $\frac{2}{\Lambda} c_{M0} = -0.058$, and for full-span

flaps, $\frac{2}{\Lambda} c_{M0} = -0.091$ and correspondingly according to

figure 19 $\frac{\partial c_{y0}}{\partial \beta} = -0.088$ and $\frac{\partial c_{y0}}{\partial \beta} = -0.049$. Admittedly

the curve $\frac{\partial c_L}{\partial \beta} (c_a)$ of the wing with 100-percent flaps diverges, like $c_M(c_a)$ within range of small c_a , considerably from a straight line and therefore the recti-

linearly extrapolated value must be taken for $\frac{\partial c_{L0}}{\partial \beta}$ exactly as for c_{M0} . Extrapolating the straight portion between $c_a \approx 0.9$ and $c_a \approx 1.5$ gives $\frac{\partial c_{L0}}{\partial \beta} \approx -0.13$

instead of -0.049 . So with this modification even the formula still is inaccurate and its application to wings with flaps is therefore very rough, quantitatively. With

50-percent flaps the rise in the straight parts of $\frac{\partial c_L}{\partial \beta} (c_a)$ is slightly less than with 100 percent flaps; on the average it is about equal to the rise of the wing without flaps.

6. Yawing moment.- For the yawing moment due to yaw of the wing without flaps the formula

$$\frac{\partial c_N}{\partial \beta} = \frac{\partial c_{N0}}{\partial \beta} - \left[\frac{2x}{\Lambda} \frac{1 + 0.15(Z - 1)}{Z + 1} + 0.084 \frac{\Lambda(1 + \sqrt{Z})}{\Lambda + 2} - 0.10 \right] \frac{c_{ag}^2}{c'_a} \quad (8)$$

gives with $x = 1.2$ a little too great a (negative) rise over c_{ag}^2 (fig. 20), as previously observed on the rectangular wing. The marked deflection of the curves near $c_a = 0$, with flaps, is certainly related with the similar phenomena observed at c_L and c_M , and might be due to separation of flow. But even in the rest of

the c_a range the curve of $\frac{\partial c_N}{\partial \beta} (c_a^2)$ is far from

straight. An explanation for it may be found in the hint given in reference 11 that on cambered profiles a term

$-(\alpha - \alpha_0) \frac{\partial c_{L0}}{\partial \beta}$, according to formula (8), should be added

to the yawing moment, because when plotted against c_a^2 this term linear in c_a would cause a curvature of the curve. Thus adding $(\alpha - \alpha_0) \frac{\partial c_{L0}}{\partial \beta}$ to the measured $\frac{\partial c_N}{\partial \beta}$ should produce a linear curve over c_a^2 , as actually is the case for the wing with 50 percent flaps according to figure 20 (aside from the irregular vicinity of $c_a = 0$). No corresponding test was made with 100 percent flaps, since it was not quite clear what value to use for $\frac{\partial c_{L0}}{\partial \beta}$.

VI. COMPARISON OF THE TEST DATA OF THE SWEEP-BACK WITH THOSE OF STRAIGHT TRAPEZOIDAL WING AND WITH THE THEORY OF THE SWEEP-BACK WING

A. Straight Air Flow

Figures 4 and 9 show the $c_a(\alpha)$, $c_a(w)$, and $c_a(c_{Mn})$ for the sweepback wing of reference (8) as dashed curves. The comparison discloses the following:

1. Without flaps (figs. 4 and 7).- At equal angle of attack the lift of the swept-back wing is smaller than that of the wing without sweepback. Near $\alpha = 0$ the swept-back wing shows $\frac{dc_a}{d\alpha} = 3.69$ and the straight wing $\frac{dc_a}{d\alpha} = 3.89$, hence a decrease of 5 percent by sweepback, while by the formula given in reference 12

$$C_{ag} = \frac{1 + \frac{c_{a'_{\infty}}}{\pi\Lambda}}{1 + \frac{c_{a'_{\infty}} \cos \varphi}{\pi\Lambda}} \cos \varphi (C_{ag})_{\varphi=0} \quad (9)$$

a decrease of 14 percent should be expected. Considering the uncertainty in the experimental determination of $\frac{dc_a}{d\alpha}$, this result agrees with the experience cited in reference 10, that experience indicates a lift decrease only half as great as formula (9).

The sweepback reduces the maximum lift coefficient by 0.13, and the related angle of attack by about 2° . However, these $c_{a_{max}}$ differences are, like the still greater differences on the wing with flaps, intimately related with the Reynolds number; they increase, at first, with increasing Re and then become smaller again (references 4 and 6). Unusual is the smoother lift decrease of the swept-back wing after exceeding the maximum lift. This is due to the separation of flow at the wing tips, where the lift loss is not so great and with increasing angle of attack progressively moves toward the center, while the straight wing breaks down fairly suddenly from the center over a large part of the span.

The polars $c_a(c_w)$ of both wings are almost identical up to near $c_{a_{max}}$, the induced drag is therefore not modified by the sweepback, which agrees with the theory within the framework of the instrumental accuracy. Theoretically, it should be 2 percent greater than on the straight wing. However, this result may not be generalized to other tapers.

On the pitching moment the dissimilar behavior after exceeding the maximum lift is of primary importance. The moment experiences an abrupt variation, nose-heavy on the straight wing, tail-heavy on the swept-back wing. The behavior of the straight wing is explained by the backward movement of the center of gravity at the flow separation, while on the swept-back wing this effect is over-balanced by the simultaneously incipient lift loss at the wing tips.

The measured neutral point of the swept-back wing lies at 0.769 mean wing chord $l_m = \frac{F}{b}$ behind $l/4$ of the wing center section. By the L-method (reference 10) the value is $a \times \frac{b}{2} = 0.4473 \times \frac{b}{2}$ for the distance of the load center of gravity of one wing half from the plane of symmetry and hence $\frac{a}{2} \Lambda \tan \phi = 0.783$ for the shifted neutral point (referred to l_m) produced by the sweepback, whereby it is to be assumed that the neutral points of the individual profile sections are not changed by the sweepback. Observing that the neutral point of the straight wing lies $0.035l_m$ before $l/4$, gives a backward position of the neutral point of 0.748 instead of the measured 0.769. That the computed point lies 2 percent l_m before the measured point might be due to the fact that the cited assumption is not entirely correct: as indicated by the pressure-distribution measurement the suction peaks in wing center are materially diminished by the sweepback, thus causing a backward shifting of the neutral point of the profile. By the Multhopp method (reference 3) we get $a = 0.4723$, $\frac{a}{2} \times \Lambda \tan \phi = 0.826$ and 0.791 for the backward position of the neutral point, hence a value 2 percent too high.

Although the profile is symmetrical, wings Nos. 1, 5, and 9 manifest at $c_a = 0$ a negative value of c_{m0} other than zero. To what this phenomenon is attributable (suspension ?) is not quite clear.

2. 100-percent flaps (figs. 6 and 9).- The sweepback reduces the zero angle of attack from -12.7° to -12.0° . Whether this is connected with the irregularities of the zero lift angle mentioned previously or whether the theoretically anticipated effect, that the zero lift angle

owing to flap deflection by sweepback is reduced by a factor ranging between 1 and $\cos \phi$ is involved, is impossible to decide. The $c_a(a)$ curves are severely curved; in the range $0 \leq a \leq 10^\circ$ we get $\frac{dc_a}{da} = 3.74$ for wing No. 5 and $\frac{dc_a}{da} = 3.34$ for wing No. 9, or a decrease of 10 percent in $\frac{dc_a}{da}$ due to sweepback, which is close to the theoretical 14 percent. The sweepback lowers the $c_{a_{max}}$ from 2.10 to 1.58. This is due in part to the decrease in $\frac{dc_a}{da}$, but in greater measure to the drop in α_{max} from 18° to 13° . The abrupt drop in c_a behind $c_{a_{max}}$ is increased on both wings by the flaps, although its magnitude on the swept-back wing is slightly less than a third of that on the straight wing. The corresponding pitching-moment variation, however, is smaller on the straight than on the swept-back wing and acts anti-stalling, while intensifying it on the swept-back wing. The polars $c_a(c_w)$ agree in the range $c_a = 0.6$ to $c_{a_{max}}$ of the swept-back wing. For small c_a the c_w of the swept-back wing is surprisingly a little higher, while theoretically the drag at zero lift should be smaller by the factor $\cos^3 \phi_K^4$ ($\phi_K =$ angle of sweepback of the flaps). For this drag is largely pressure drag from the dead air region behind the flaps and hence perpendicular to the flaps; the projection on the wind direction gives a factor $\cos \phi_K$ and the reduction of the effective airspeed by $\cos \phi_K$ a factor $\cos^2 \phi_K$.

3. 50-percent flaps (figs. 5 and 8).- The sweepback reduces the $c_{a_{max}}$ from 1.7 to 1.35, due essentially to the decrease in α_{max} from 18° to 14° . The moment variation on the swept-back wing with part-span flaps (50 percent) is considerably less than on that with full-span flaps and even a little smaller than without flaps, but also in the sense of increasing angle of attack.

⁴It actually should be considered that the flaps even on the wing without sweepback assume a certain swept-back setting.

The induced drag of the swept-back wing is appreciably smaller than that without sweepback. This is readily apparent when considering that the sweepback reduces the lift accumulation produced by the flaps in wing center in the sense of an approach to the elliptic lift distribution.

B. Yawed Flow

1. Lift.— The lift of the swept-back wing in yaw without flaps follows the law $\cos^2\beta$ very closely, figure 22. But with flaps considerable departure from $\cos^2\beta$ occurs, in contrast to wing No. 5. This is due to the fact that the swept-back wing with flaps exhibits certain additive effects in yaw which do not occur on the straight wing and which are essentially due to the fact that on the swept-back wing the angle of attack is not adjusted by rotation about the $l/4$ line as on the straight wing. Namely, according to reference (12)

$$C_a = \cos^2\beta \times C_{ag} + \frac{1 + \frac{c_{a'}\omega \cos \varphi}{\pi\Lambda}}{1 + 2 \frac{c_{a'}\omega \cos \varphi}{\pi\Lambda}} \tan^2\varphi \times \sin^2\beta (C_{ag})_{\alpha=0} \quad (10)$$

From this it follows that without flaps the law $\cos^2\beta$ applies, and that for flap deflection, where the lift for $\alpha = 0$ does not disappear, the lift of the swept-back wing does not remain zero, when, starting from zero lift in straight flow, the yaw is begun with constant angle of attack.

Figure 25 represents the theoretical curves (according to reference 10) for the swept-back wing without, with 50-percent and with 100-percent flaps, along with the related test points. Aside from the maximum angles of attack (separation of flow) the agreement in the first and last case is very good; that it is less good for 50-percent flaps is not surprising, since formula (10) was not developed for this case (the second summand should be reduced on account of induction).

2. Drag.- A comparison of $\frac{c_w}{c_{wg}}$ in figures 21 and 22 manifests on the swept-back wing considerable departure from the $\cos^2\beta$ curve, due probably to instrumental inaccuracy, while with flaps the test points are comparatively well placed on the $\cos\beta$ curve, especially for smaller angles of attack. Considering that at zero lift the drag is largely pressure drag caused by the flaps, hence is perpendicular to the flaps, and denoting the drag coefficient of a profile section perpendicular to the flap with c_w^* , the drag (measured in wind direction) of the yawing swept-back wing with 100-percent flaps is at small c_a

$$\begin{aligned} c_w &= \frac{1}{2} \left[\cos^3(\varphi_K - \beta) + \cos^3(\varphi_K + \beta) \right] c_w^* \\ &= (\cos^3\varphi_K \cos^3\beta + 3 \cos\varphi_K \cos\beta \sin^2\varphi_K \sin^2\beta) c_w^* \\ &= \cos\beta \left[1 + (3 \tan^2\varphi_K - 1) \sin^2\beta \right] c_{wg} \end{aligned} \quad (11)$$

if φ_K is the angle of sweepback of the flaps and c_{wg} the drag coefficient in straight air flow (and equal angle of attack). For wing No. 9, $\tan\varphi_K = 0.554$, so that the brackets are almost equal unity, hence $\frac{c_w}{c_{wg}} \approx \cos\beta$. With increasing angle of attack the induced drag then increases, probably as $\cos^2\beta$, so that c_w/c_{wg} shifts from $\cos\beta$ toward $\cos^2\beta$. This actually is the case for 100-percent flaps⁵; for 50-percent flaps the conditions are more complicated on account of the induced drag existing at $c_a = 0$.

3. Pitching moment.- A glance at figure 24 shows that the pitching moment does not vary with $\cos^2\beta$ in yaw. This is particularly evident with flaps. But by theory itself another law must be applicable with flaps: With $c_{m_0}^*$ as the zero moment of a profile section

⁵It is a peculiar fact that the relationship $c_w = \cos^3\varphi_K c_w^*$ following from the same argument for zero lift drag of swept-back and straight wing is not substantiated by the measurement.

perpendicular to the $l/4$ line, the zero moment c_{M0} of the swept-back wing with full-span flaps in yaw is

$$\begin{aligned} c_{M0} &= \frac{1}{2} \left[\cos^2(\varphi - \beta) + \cos^2(\varphi + \beta) \right] c_{M0}^* \\ &= (\cos^2\varphi \cos^2\beta + \sin^2\varphi \sin^2\beta) c_{M0}^* \end{aligned} \quad (12)$$

and with the introduction of the term $c_{M0g} = \cos^2\varphi \times c_{M0}^*$ resulting for $\beta = 0$

$$c_{M0} = (\cos^2\beta + \tan^2\varphi \sin^2\beta) c_{M0g} \quad (13)$$

that is, the zero moment is varied by the yaw by the summand

$$c_{M0} - c_{M0g} = c_{M0g} (\tan^2\varphi - 1) \sin^2\beta \quad (14)$$

Starting to yaw from zero lift in straight flow at constant angle of attack the expression (13) does by no means represent the complete pitching moment, since the lift by reason of (10) does not remain zero in yawing and therefore contributes to the moment. So when assuming that the neutral-point position x_N (eventually dependent on c_a) does not vary in yaw the total difference of the pitching moment in yaw and for straight flow is

$$\begin{aligned} c_M(\alpha) - c_{Mg}(\alpha) &= c_{M0g} \times (\tan^2\varphi - 1) \sin^2\beta + x_N (c_a - c_{ag}) \\ &= c_{M0g} (\tan^2\varphi - 1) \sin^2\beta + c_{Mg}(c_a) - c_{Mg}(c_{ag}) \end{aligned} \quad (15)$$

hence, owing to $c_{Mg}(\alpha) = c_{Mg}(c_{ag})$

$$c_M = c_{Mg}(c_a) + c_{Mag}(\tan^2\phi - 1)\sin^2\beta \quad (16)$$

Thus the moment⁶ for wing No. 9 with 100-percent flaps in yaw is obtained by taking the lift coefficient c_a existing in yaw from the measurement or else compute it by formula (10), read the moment $c_{Mg}(c_a)$ related to this c_a for straight flow from figure 6 (dashed curve) and add the second term of (16), c_{Mag} itself being taken from figure 6 also. The result of this calculation, shown in figure 24 in comparison with the measurement, is in good agreement.

Theoretically the moment of the swept-back wing without flaps should behave as $\cos^2\beta$, with an additive term for 50-percent flaps. But in view of the irregular variation of the measured curves no detailed study was made.

4. Transverse force, cross-wind force.— The coefficient of stability $\frac{\partial c_y}{\partial \beta}$ of the cross-wind force for both wings is reproduced in figure 27. Owing to the comparatively great instrumental inaccuracy no information concerning the effect of sweepback on the smooth wing was obtained. However, the marked shift of $\frac{\partial c_y}{\partial \beta}$ to positive values as a result of flap deflection on the swept-back wing should be real.

This shift can be explained as follows: With c_{*WD} denoting the coefficient of pressure drag of the flaps (at right angle to the flaps), the coefficient of the cross-wind force at zero lift is

$$\begin{aligned} c_{y0} &= c_{*WD} \frac{1}{2} \left[\cos^2(\phi_K - \beta) - \cos^2(\phi_K + \beta) \right] \sin \phi_K \\ &= 2c_{*WD} \cos \phi_K \sin^2 \phi_K \sin \beta \cos \beta \end{aligned} \quad (17)$$

⁶Since the formula applies to any reference point, the subscript n was omitted.

and, since by (11) in straight flow (friction drag discounted) $c_{wog} = c_{*WD}^3 \cos^3 \varphi_K$

$$\frac{\partial c_{y0}}{\partial \beta} = 2 \tan^2 \varphi_K c_{wog} \quad (18)$$

On wing No. 9 with 100-percent flaps $\tan \varphi_K = 0.554$ and $c_{wog} = 0.128$, hence $\frac{\partial c_{y0}}{\partial \beta} = 0.069$, a value to some extent in agreement with the measurement. Theoretically there is another additive constituent which is based on phenomena similar to the lift variation and which for the wing in question is about of the same order of magnitude as the effect (18), so that, speaking as a whole, there is no agreement between theory and test.

Figure 26 gives the stability coefficient $\frac{\partial c_g}{\partial \beta}$ of the transverse force against c_{ag}^2 for both wings. Without flaps there is no difference in the unstalled flow regime, the agreement with the theory according to (4) is very good even for wing No. 9. But with flaps the transverse force of the swept-back wing is substantially less than that of the straight wing, even though the drag is not essentially different, so that the formula (4) cannot be quite correct for the swept-back wing. This is fairly evident because of the relation for the transverse force of the swept-back wing with flaps at zero lift

$$c_{go} = c_{*WD}^2 \frac{1}{2} \left[\cos^2(\varphi_K - \beta) \sin(\varphi_K - \beta) - \cos^2(\varphi_K + \beta) \sin(\varphi_K + \beta) \right] \quad (19)$$

hence

$$\frac{\partial c_{go}}{\partial \beta} = c_{*WD}^3 \cos^3 \varphi_K (2 \tan^2 \varphi_K - 1) = c_{wog} (2 \tan^2 \varphi_K - 1) \quad (20)$$

and therefore

$$\frac{\partial c_{g0}}{\partial \beta} = -0.59$$

A value in agreement with the measurements. (For the comparison the straight part on $c_a = 0$ must be extrapolated.) Further discussion of the c_a curve would involve the induction which is omitted. Strictly empirical it may be said that a practical agreement with the measurement is obtained by adding the measured $c_{wog} - c_{wg}$ to (20).

5. Rolling moment.- Figure 28 shows the rolling moment due to yaw of the swept-back and the straight wing compared with the theory according to (12). The recorded $\frac{\partial c_L}{\partial \beta}$ values of the swept-back wing are connected by curves, while dotted lines of the interpolation are placed through the test point of the straight wing and which is the same straight line for both the 50-percent and the 100-percent flaps. Whereas the slope of $\frac{\partial c_L}{\partial \beta}$ for wing No. 5 is about the same with and without flaps, it is appreciably weaker for the swept-back wing with 100-percent flaps than the nearly agreeable slope with and without 50-percent flaps. The behavior of $\frac{\partial c_L}{\partial \beta}$ at $c_a = 0$ is unusual. While the values of the straight and the swept-back wing without and with 50-percent flaps agree, they are far apart for the 100-percent flaps, even to a change in prefix. These phenomena are related with the effect of flap deflection on the swept-back wing already discussed for the lift, and can be theoretically explained.

Reference 12 contains two formulas derived for the rolling moment due to yaw as a result of sweepback, one with induction disregarded but for any flap width

$$\frac{\partial c_{Lpf}}{\partial \beta} = 0.44 \tan \phi \left[c_{ag} + (2\bar{y}_0 - 1) (c_{ag})_{\alpha=0} \right] \quad (21)$$

the other with the induction allowed for, but which holds only for without and with 100-percent flaps:

$$\frac{\partial c_{Lpf}}{\partial \beta} = 0.44 \tan \phi \left[\left(1 + \frac{\frac{c_{a'} \cos \phi}{\pi \Lambda}}{1 + 2 \frac{c_{a'} \cos \phi}{\pi \Lambda}} \right) c_{ag} + \frac{1 + \frac{c_{a'} \cos \phi}{\pi \Lambda}}{1 + 2 \frac{c_{a'} \cos \phi}{\pi \Lambda}} (c_{ag})_{\alpha=0} \right] \quad (22)$$

with $(c_{ag})_{\alpha=0}$ denoting the lift coefficient existing at $\alpha = 0$ (and $\beta = 0$), so that this term disappears for the wing without flaps. The flaps reach from wing center to $\bar{y}_0 \times \frac{b}{2}$, hence $\bar{y}_0 = 0.5$ for 50-percent flaps, and $\bar{y}_0 = 1$ for 100-percent flaps. The formulas give only the sweepback portion, so must be added to the $\frac{\partial c_L}{\partial \beta}$ of the straight wing (dotted line in fig. 28), to give the total moment of the swept-back wing.

There is no very great difference between the formulas with and without induction. The slope of the recorded curves without and with 50-percent flaps is very closely reproduced by the theory; why the slope for 100-percent flaps diminishes is not clear. The behavior at $c_a = 0$ is also very well described by the theory, while the statement (made in reference 12) that the rolling moment due to yaw as a result of sweepback is twice as high for $\alpha = 0$ than for $c_a = 0$ is also proved correct.

6. Yawing moment.— The stability factors $\frac{\partial c_n}{\partial \beta}$ of the swept-back and the straight wing are contrasted in figure 29. In all three cases the restoring moment is increased by sweepback, which is, largely by an increase in the negative slope of $\frac{\partial c_n}{\partial \beta}$ relative to c_{ag}^2 .

The theoretical yawing moment due to yaw as a result of sweepback (reference 12) on the wing without flaps is

$$\frac{\delta c_{npf}}{\delta \beta} = -0.44 \tan \varphi \frac{c_{ag}^2}{c_a'} \left[1 + \frac{\frac{c_a' \infty \cos \varphi}{\pi \Lambda}}{1 + 2 \frac{c_a' \infty \cos \varphi}{\pi \Lambda}} \left(1 - \frac{2/\cos^2 \varphi}{1 + \frac{c_a' \infty \cos \varphi}{\pi \Lambda}} \right) \right] \quad (23)$$

a formula that yields too small amounts for wing No. 9 according to figure 29. The lever arm 0.44 applicable to lift distribution should probably be replaced by a higher value for the yawing moment.

The comparison with theory for the wing with flaps is omitted in view of the same difficulties as encountered for transverse and cross-wind force.

C. Maximum Lift and Pitching Behavior

1. Maximum lift.- Figure 30 represents the correlated $c_{a_{max}}$ data of wings Nos. 5 and 9 (from reference 8). It indicates the unfavorable effect of the sweepback which, within the explored Re range is fairly independent of the Reynolds number, but on the whole is nevertheless greatly affected by it, the differences between straight and swept-back wing increase at first with increasing Re , then become smaller again (references 4 and 6). Regarding further $c_{a_{max}}$ data on wing No. 9 with landing aids, reference 9 should be consulted.

2. Pitching behavior.- The pitching action of the straight and the swept-back trapezoidal wing was investigated by a method suggested by Liebe (reference 2), whereby a run was made at an angle of attack near $c_{a_{max}}$ over the angle of yaw. From the abrupt variations in the coefficients, especially the rolling moment due to yaw are subjected, certain deductions can be made, about the probable pitching characteristics of the wing with the admittedly restrictive remark that the behavior of the coefficients in the presence of fuselage, nacelles, etc., may change fundamentally and that the study of individual

stationary coefficient measurements gives but a very rough picture, since the actual pitching process is the complicated (nonstationary) interaction of all six components.

The data from the pitching measurements on wing No. 5 are given in figures 31 to 34. The angle $c_{a_{max}}$ served as angle of attack⁷. One measurement (fig. 32) was made closely behind $c_{a_{max}}$. Figures 32 to 34 contain two independent measurements, one made by proceeding from the (almost) sound state at $\beta = 0$ and equal angle of attack in direction of positive angles of yaw, the other in direction of negative angles of yaw. The latter measurement is indicated by dashes. This contrast of two measurements and the gradually perceptible symmetry of the variations (the occasional dissimilarity in the angle being disconnected) indicates that the behavior is not accidental but subject to a certain law, and hence embodies a characteristic of the wing.

On comparing the measurements of the straight with those of the swept-back wing (reference 8, figs. 22 to 27) the difference in the behavior of c_a and c_m is apparent: on the straight wing the flow separates first in the center and causes a great variation in c_a and a nose-heavy variation in c_m , while on the swept-back wing the flow separates first at the tips and shows small c_a variations and tail-heavy variations in c_m . The variations in the rolling moment due to yaw which presumably determine the pitching behavior most are a little greater on the swept-back than on the straight wing, but the difference is not as great as might be expected perhaps on the basis of the differently located breakdown zones. The explanation for it is that, while on the swept-back wing the lever arm of the additional force created by the separation is greater, the force itself is smaller than on the straight wing, as proved by the c_a curve.

On both wings the mounting of flaps causes an increase in the variations.

⁷As is known $c_{a_{max}}$ depends on the temperature and barometric pressure of the wind, but even at equal state the values are not always definitely reproducible. This explains the minor $c_{a_{max}}$ differences found when comparing the different diagrams of the present report,

A minor dissimilarity, although perhaps of no great significance in both wings is that the transverse force of the straight wing is always near zero for straight flow even in the separated state, while it can assume fairly high values on the swept-back wing, especially when fitted with flaps. The reason for it is clear: on the straight wing the resultant force of half the wing is parallel to the plane of symmetry at $\beta = 0$, and therefore parallel to the wind, while on the swept-back wing it is largely perpendicular to the local $l/4$ line and so can furnish a component perpendicular to the wind.

Summing up it may be presumed on the basis of the discussed measurements, that the swept-back wing by reason of the somewhat greater variation in rolling moment due to yaw and the stalling acting variation in pitching moment is more unfavorable than the straight wing, aside from its substantially inferior aileron effect.

Translation by J. Vanier
National Advisory Committee
for Aeronautics

REFERENCES

1. Busmann/Kopfermann: Sechskomponentenmessungen an Rechteckflügeln mit verschiedenem Seitenverhältnis. UM 2028.
2. W. Liebe: Ergebnisse von Abkippmessungen. Ein meßtechnisch einfaches Verfahren zur Bestimmung von Abkippeigenschaften am Modell. FB 1200/2.
3. H. Multhopp: Die Anwendung der Tragflügeltheorie auf Fragen der Flugmechanik. Bericht S2 der Lilienthal-Ges.f.Luftf.-Forschg. S.53.
4. H. J. Puffert: Dreikomponentenwindkanalmessungen an gepfeilten Flügeln und an einem Pfeilflügel-Gesamtmodell. FB 1726.
5. H. J. Rautenberg: Die gegenseitige Kopplung der flugmechanischen Achsenkreuze. Luftf.-Forschg. Bd. 17 (1940), S.106.
6. Saliger: Auftriebsmessungen an einem 35° rückgepfeilten Flügel im Windkanal von Chalais Meudon (erscheint demnächst).
7. G. Thiel/J. Weissinger: Sechskomponentenmessungen an einem Rechteckflügel ohne und mit Spreizklappen. FB 1729.
8. G. Thiel/J. Weissinger: Sechskomponentenmessungen an einem 35° rückgepfeilten Trapezflügel ohne und mit Spreizklappen. UM 1152.
9. G. Thiel/J. Weissinger: c_{amax} -Messungen an einem 35° rückgepfeilten Trapezflügel mit verschiedenen Landehilfen. UM 1101.
10. J. Weissinger: Über die Auftriebsverteilung von Pfeilflügeln. FB 1553.
11. J. Weissinger: Ergänzungen und Berichtigungen zur Theorie des schiebenden Flügels. Jahrbuch 1943 der Dtsch.Luftf.-Forschg. (Vorabdruck in Technische Berichte Bd.10 (1943), Heft 7).

12. J. Weissinger: Bemerkungen über Kräfte und Momente des schiebenden Tragflügels. (Erscheint demnächst).

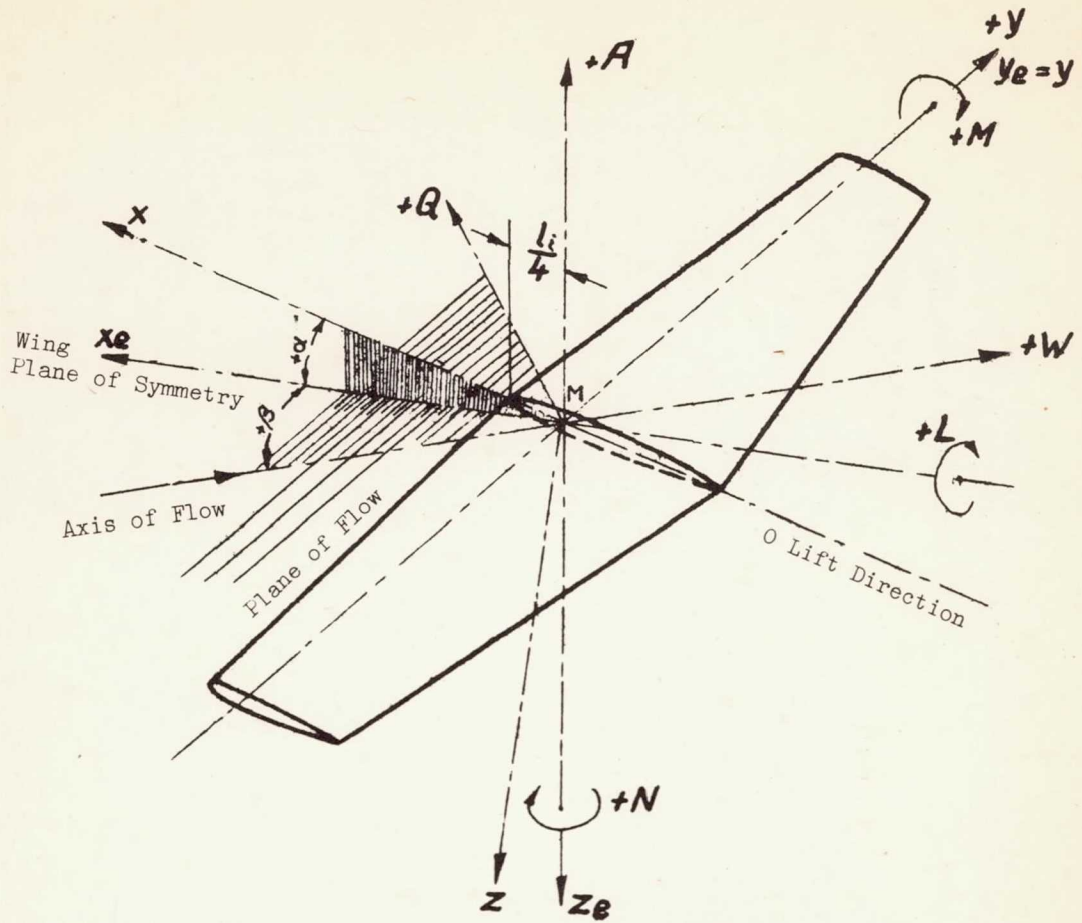


Figure 1. System of coordinates

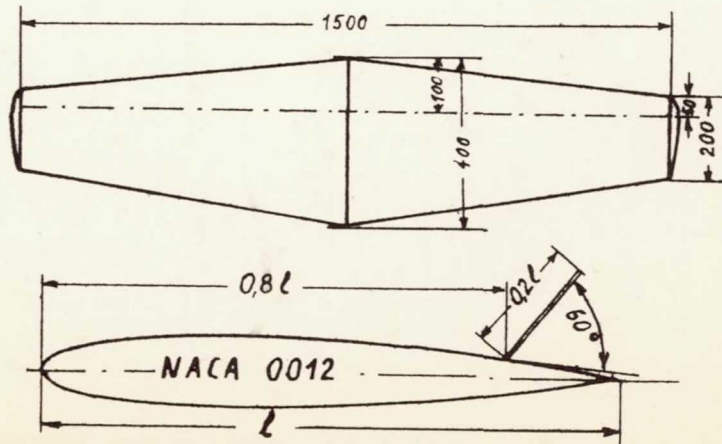


Figure 2. Dimensions of model—wing No. 5

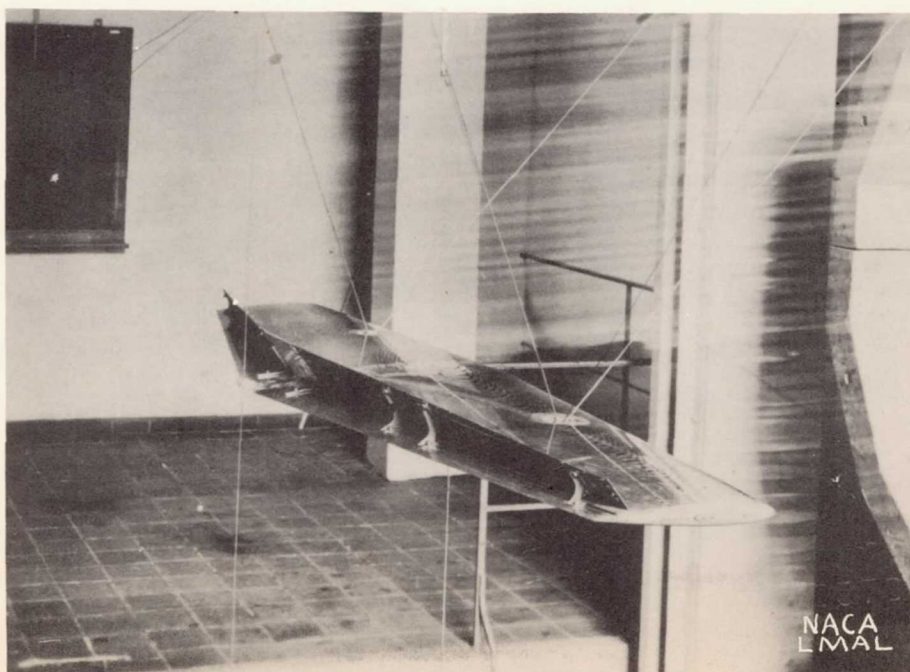
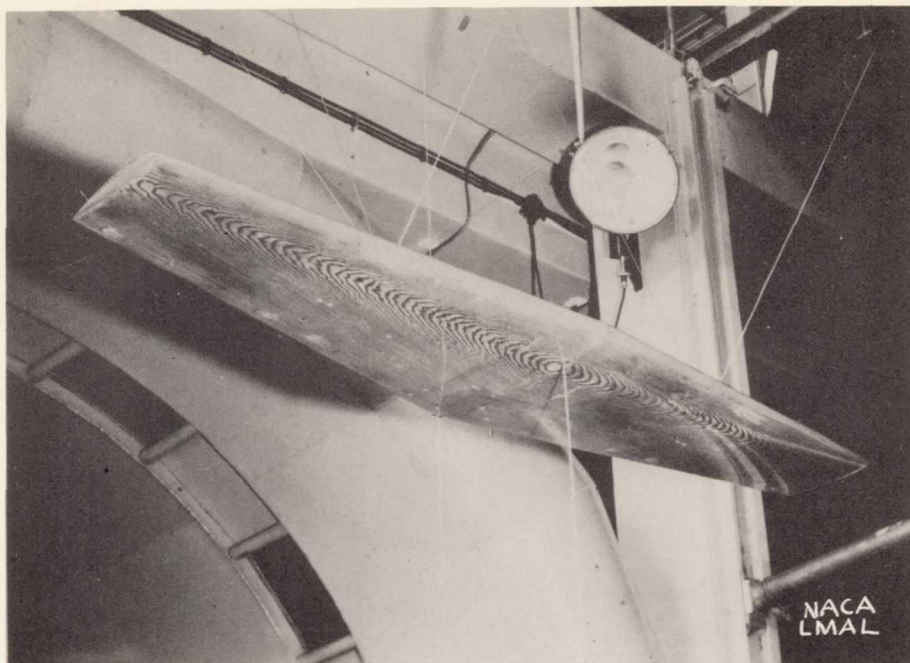
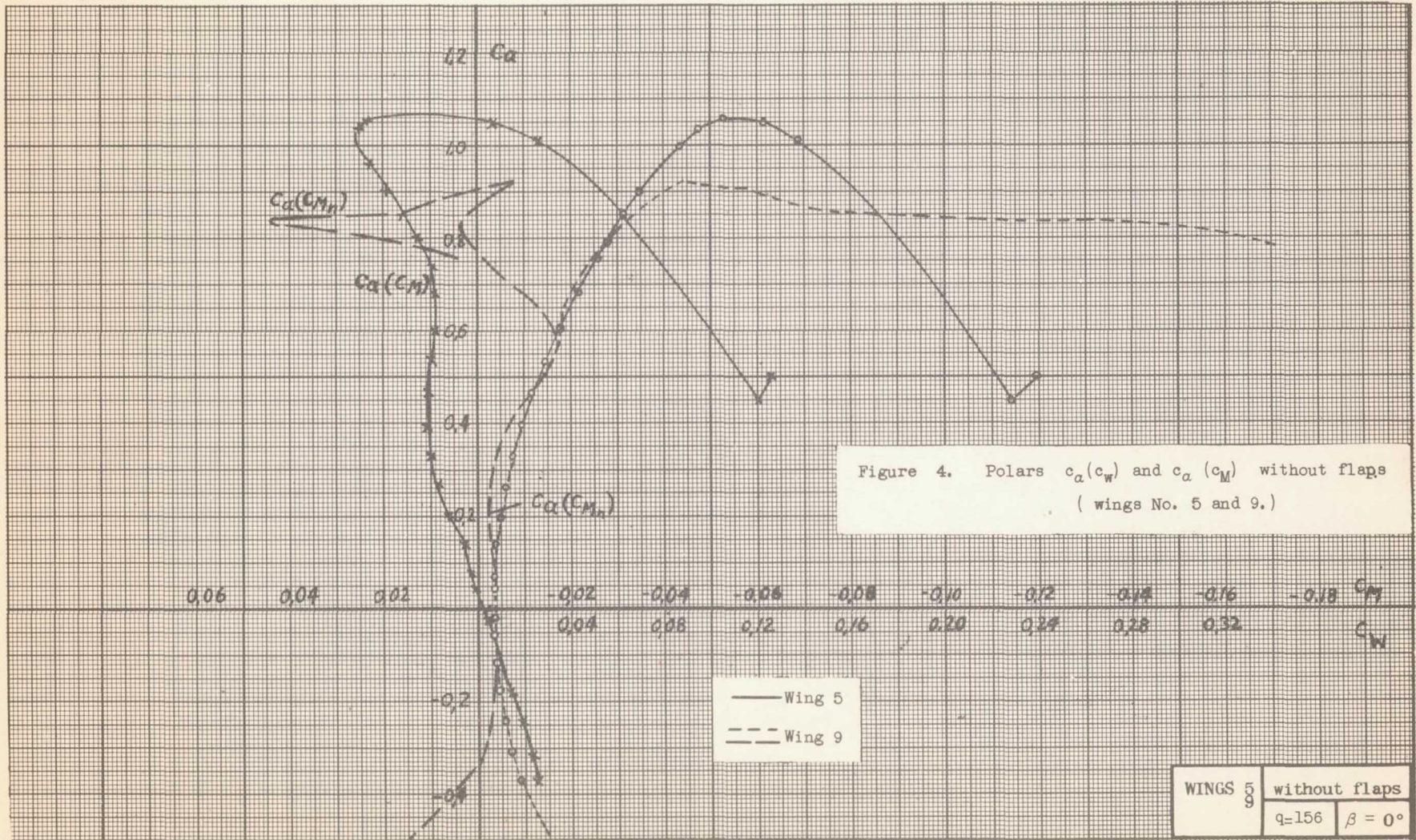


Figure 3. Wing No. 5 with full-span (100%) split flaps



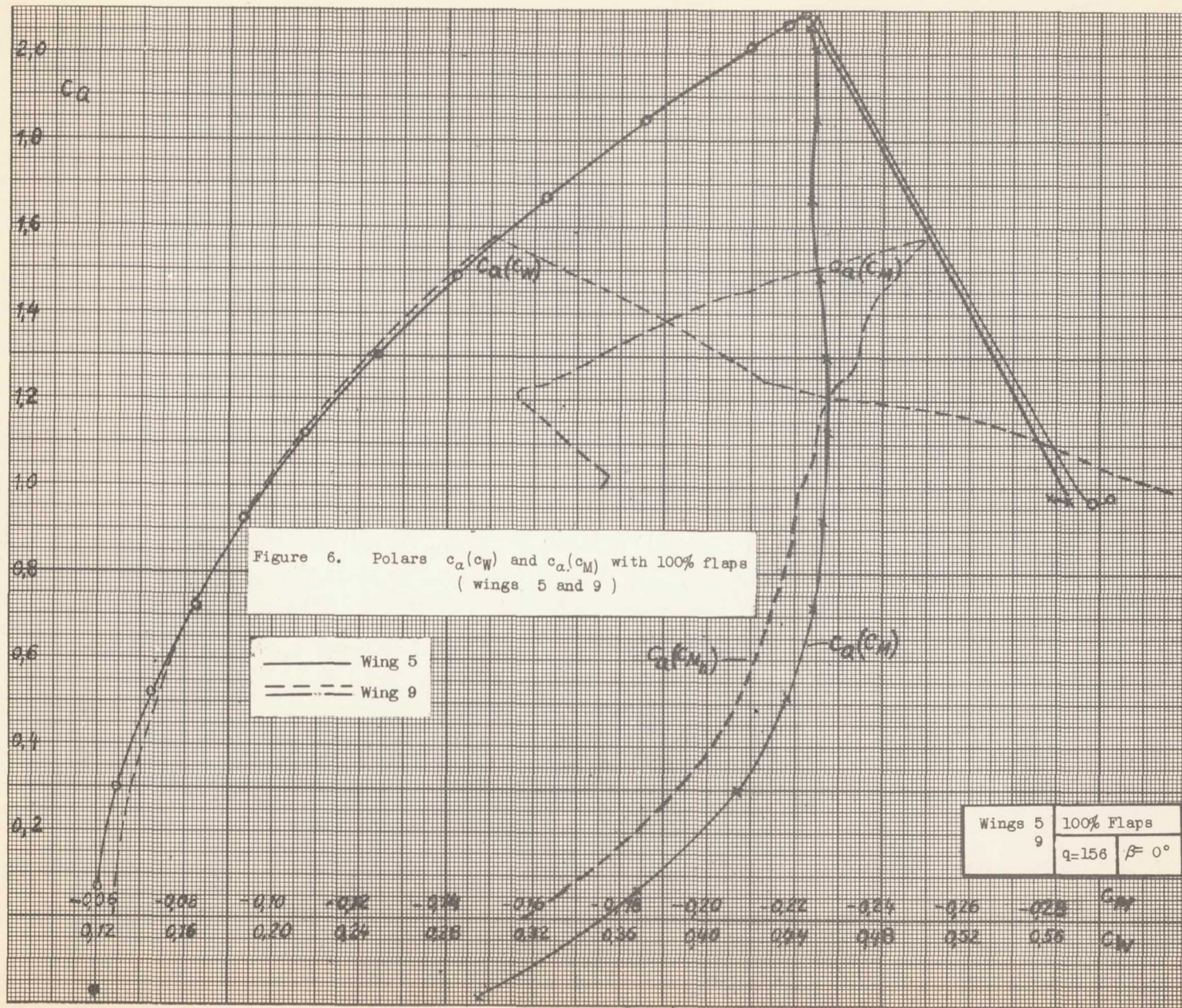
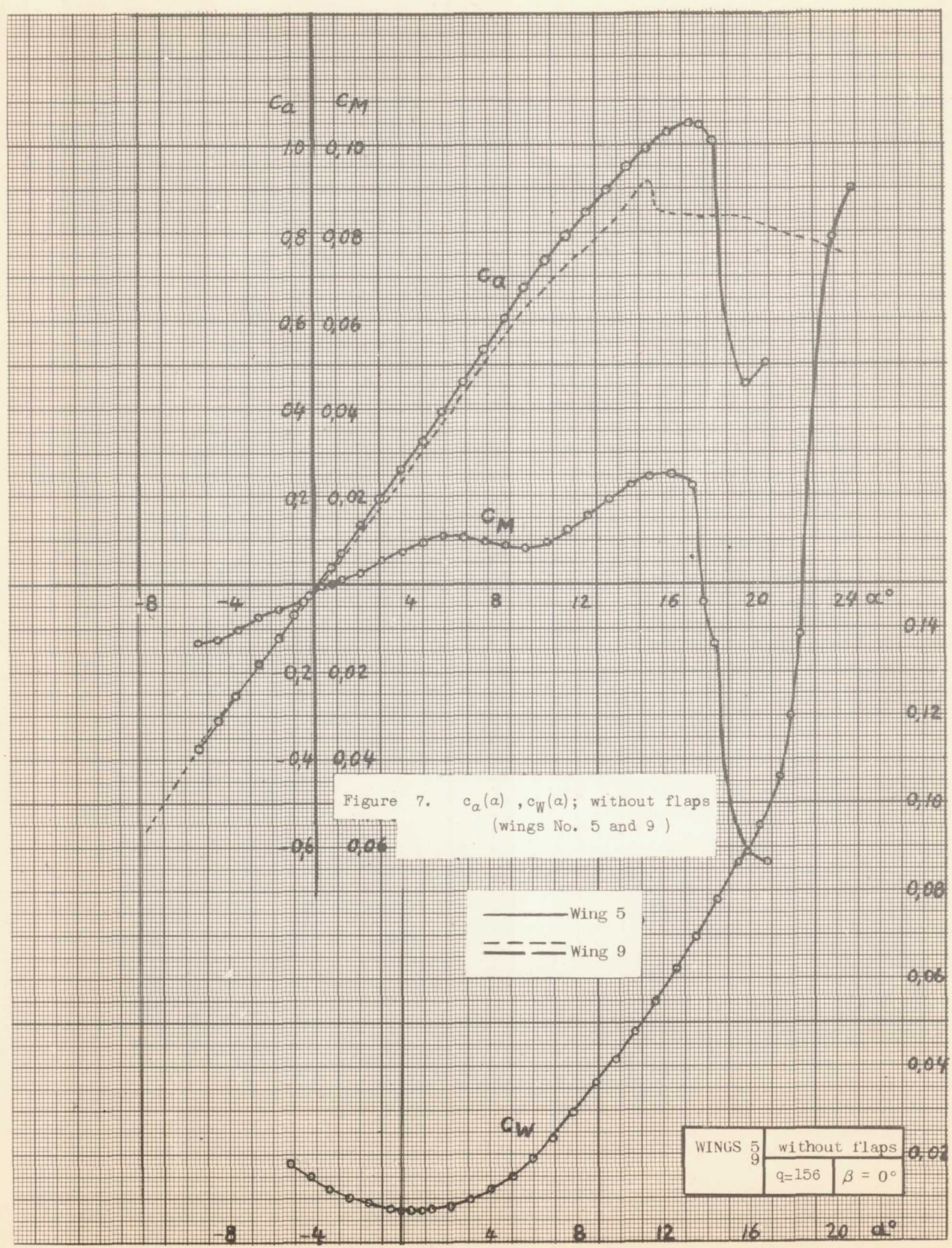
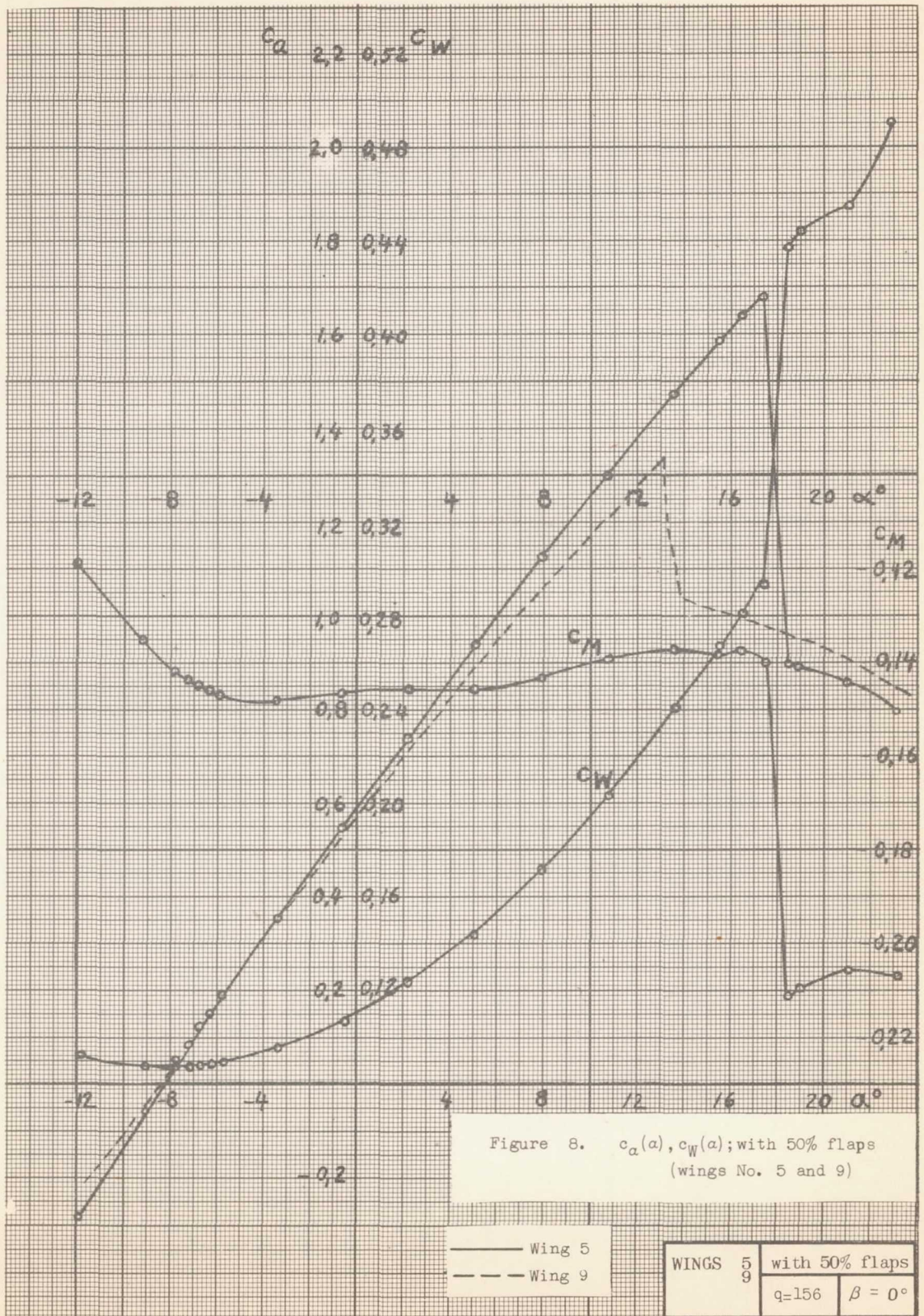
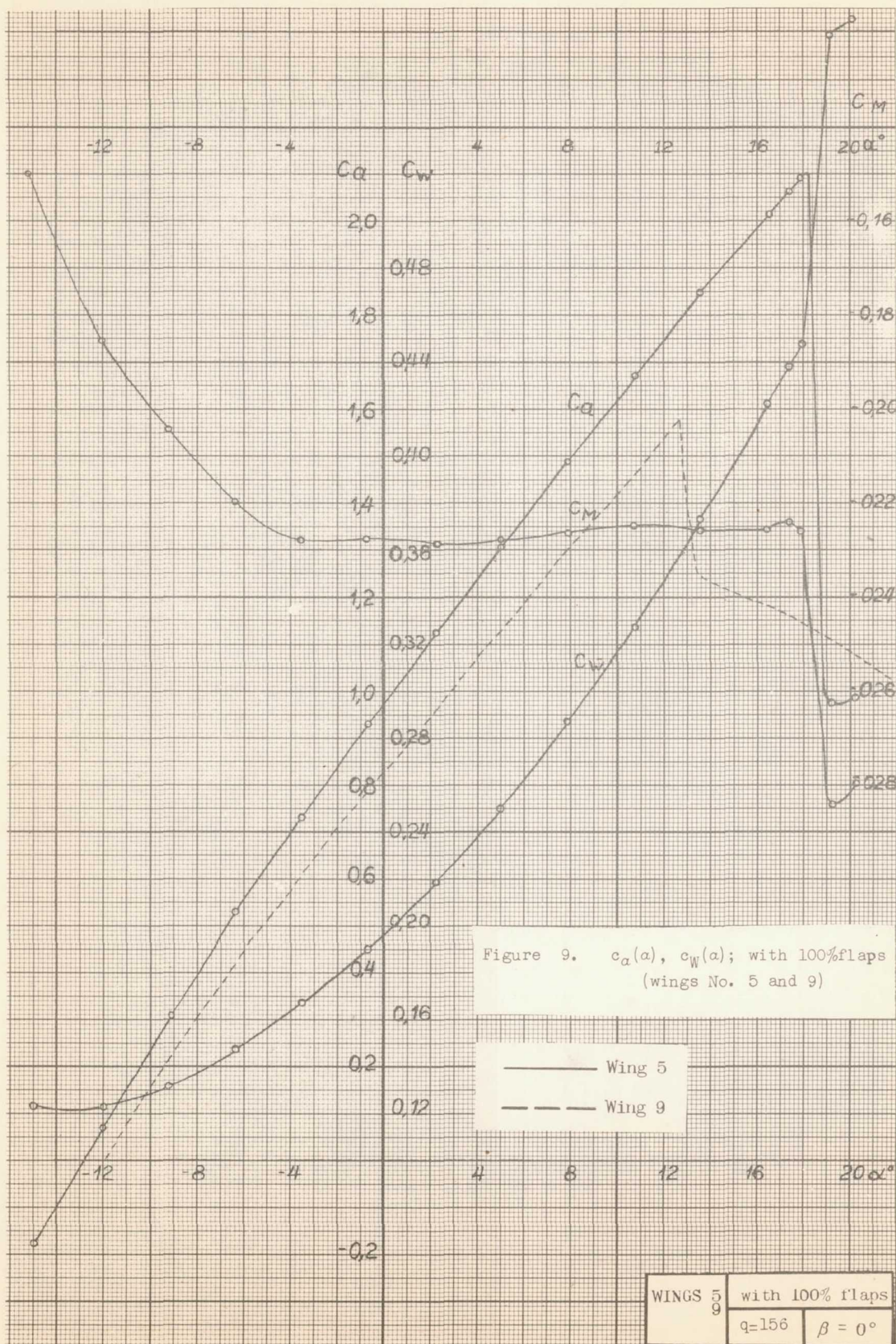
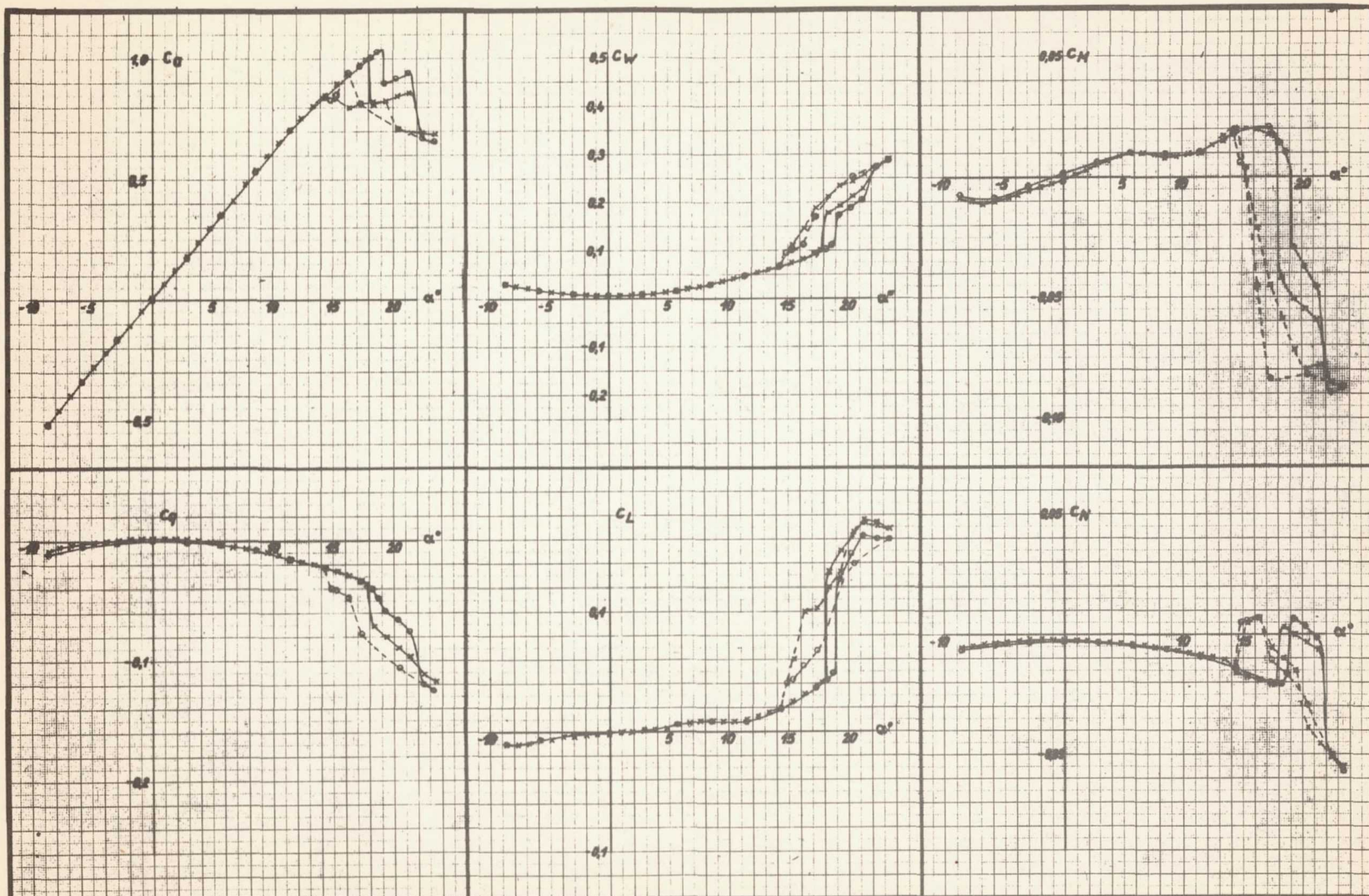


Fig. 6





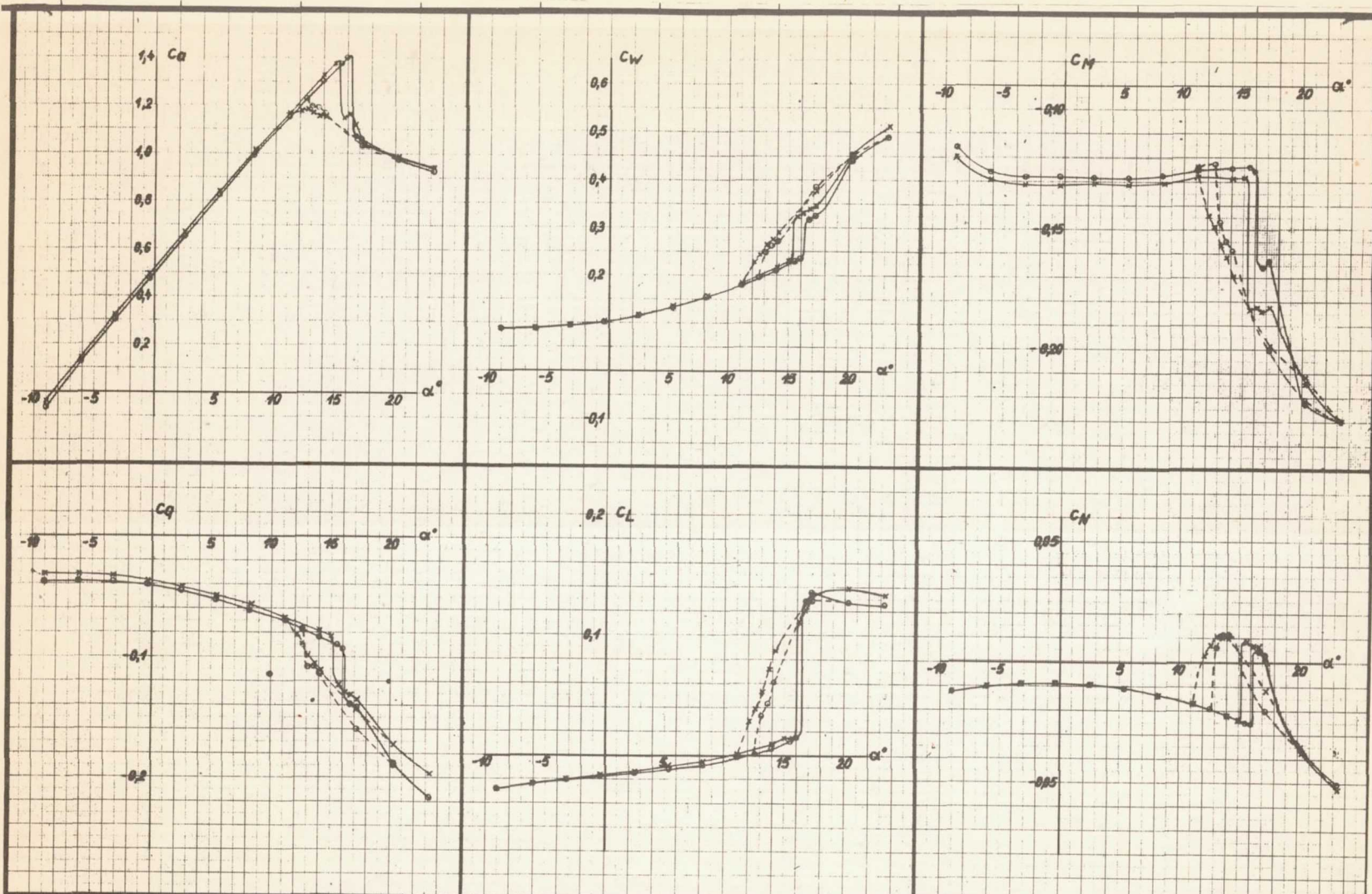




Wing 5 modified wing tips
 without flaps $q = 156$
 $\beta = +20^\circ - \circ$ $\beta = -20^\circ - \times$

Figure 10. The 6 coefficients plotted against α at $\beta = \pm 20^\circ$; wing No. 5 without flaps.

For $\beta = 20^\circ$ at c_q, c_L, c_N the sign is to be inverted

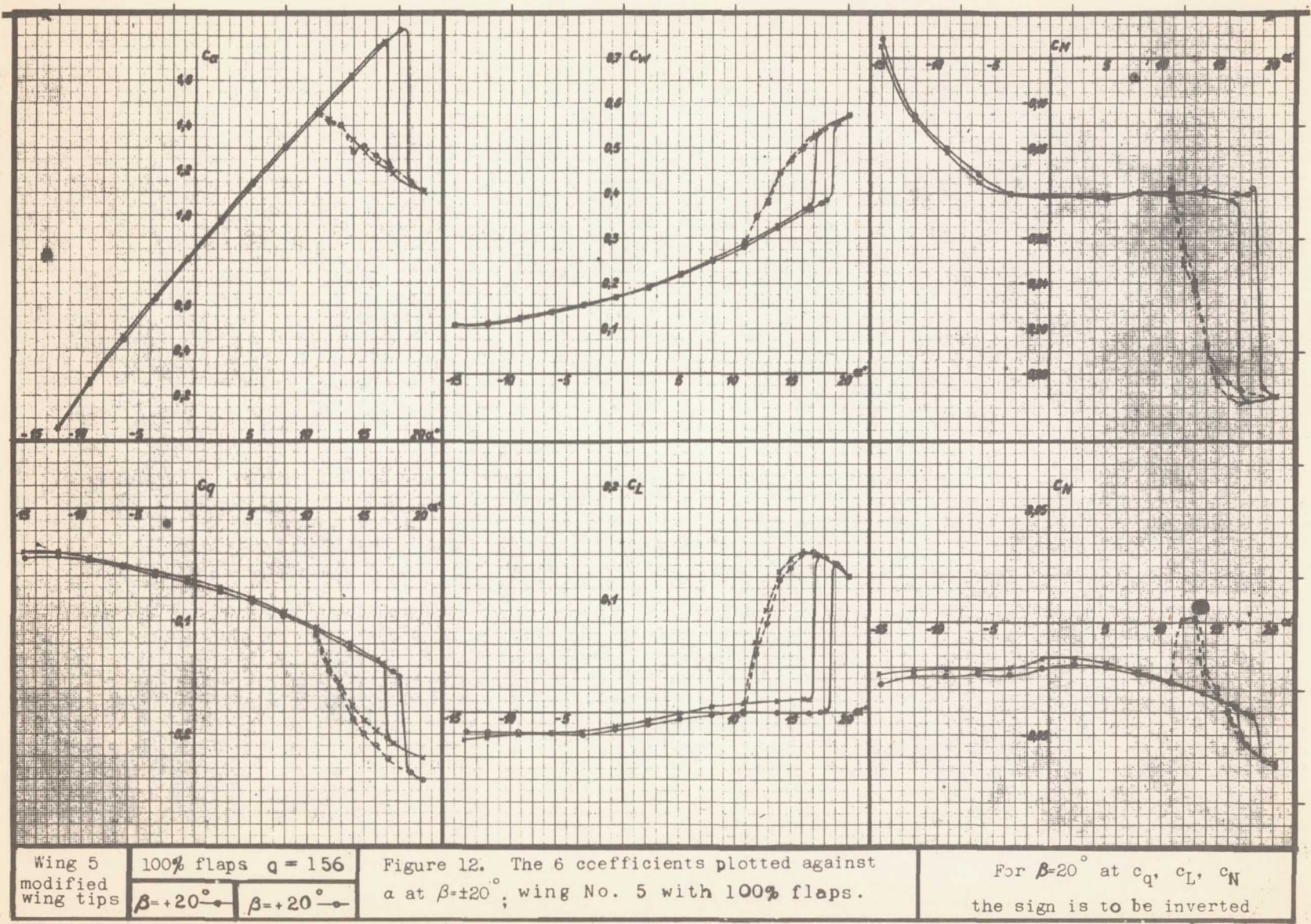


Wing 5
modified
wing tips

50% flaps	$q = 156$
$\beta = -20^\circ$	$\beta = -20^\circ$

Figure 11. The 6 coefficients plotted against α at $\beta = \pm 20^\circ$; wing No. 5 with 50% flaps.

For $\beta = 20^\circ$ at c_q, c_L, c_N
the sign is to be inverted



Wing 5
modified
wing tips

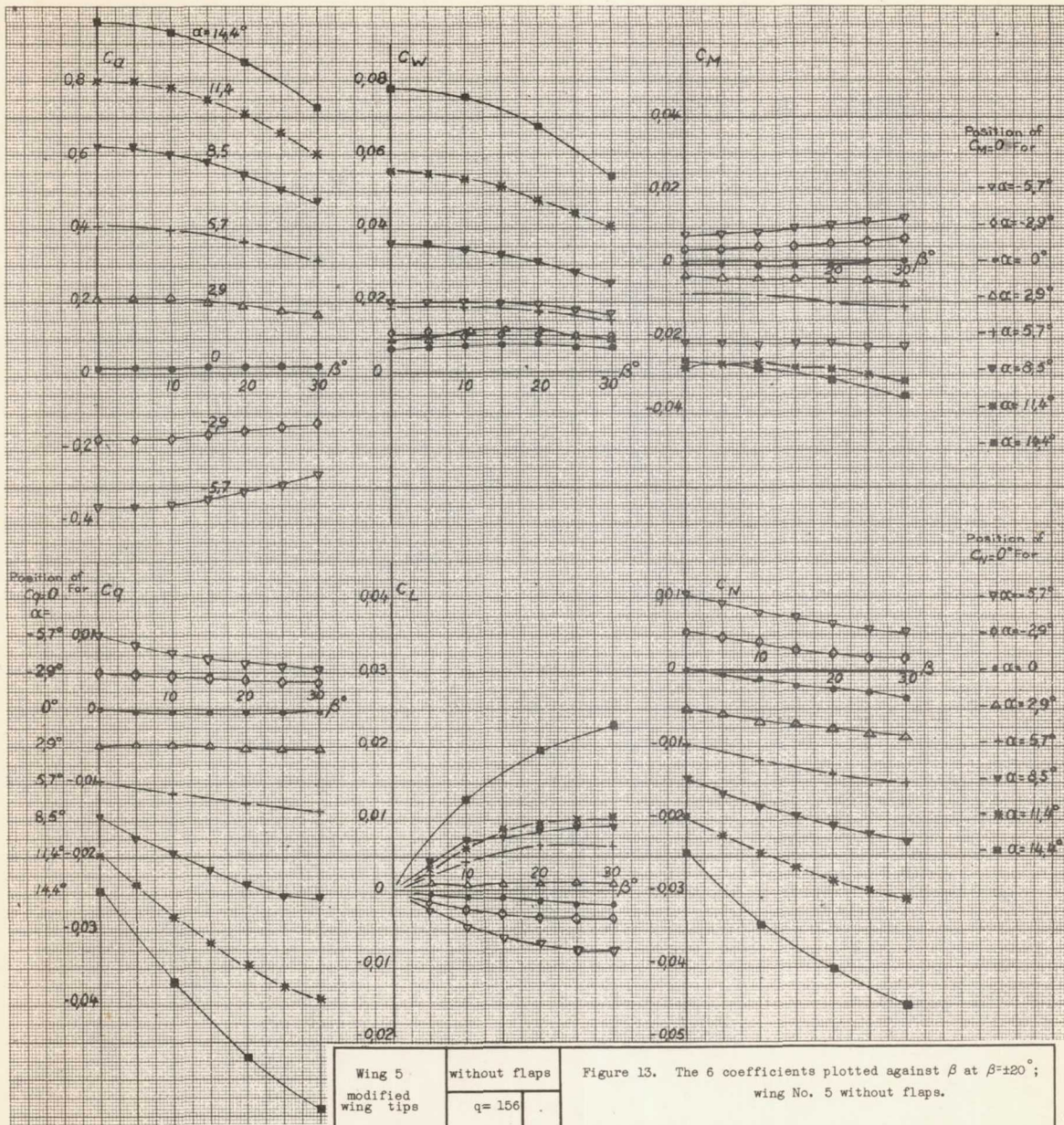
100% flaps $q = 156$

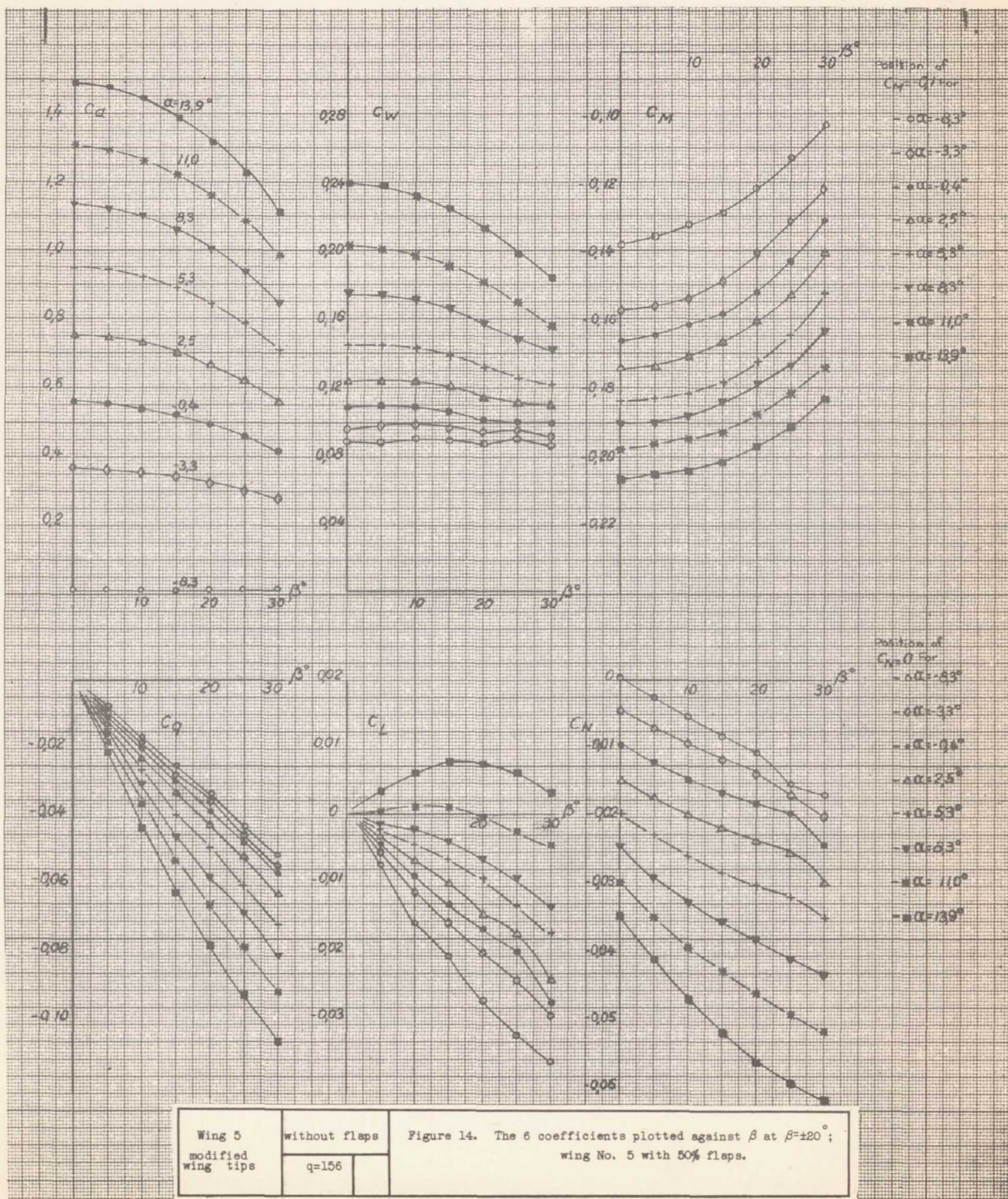
$\beta = +20^\circ$ $\beta = -20^\circ$

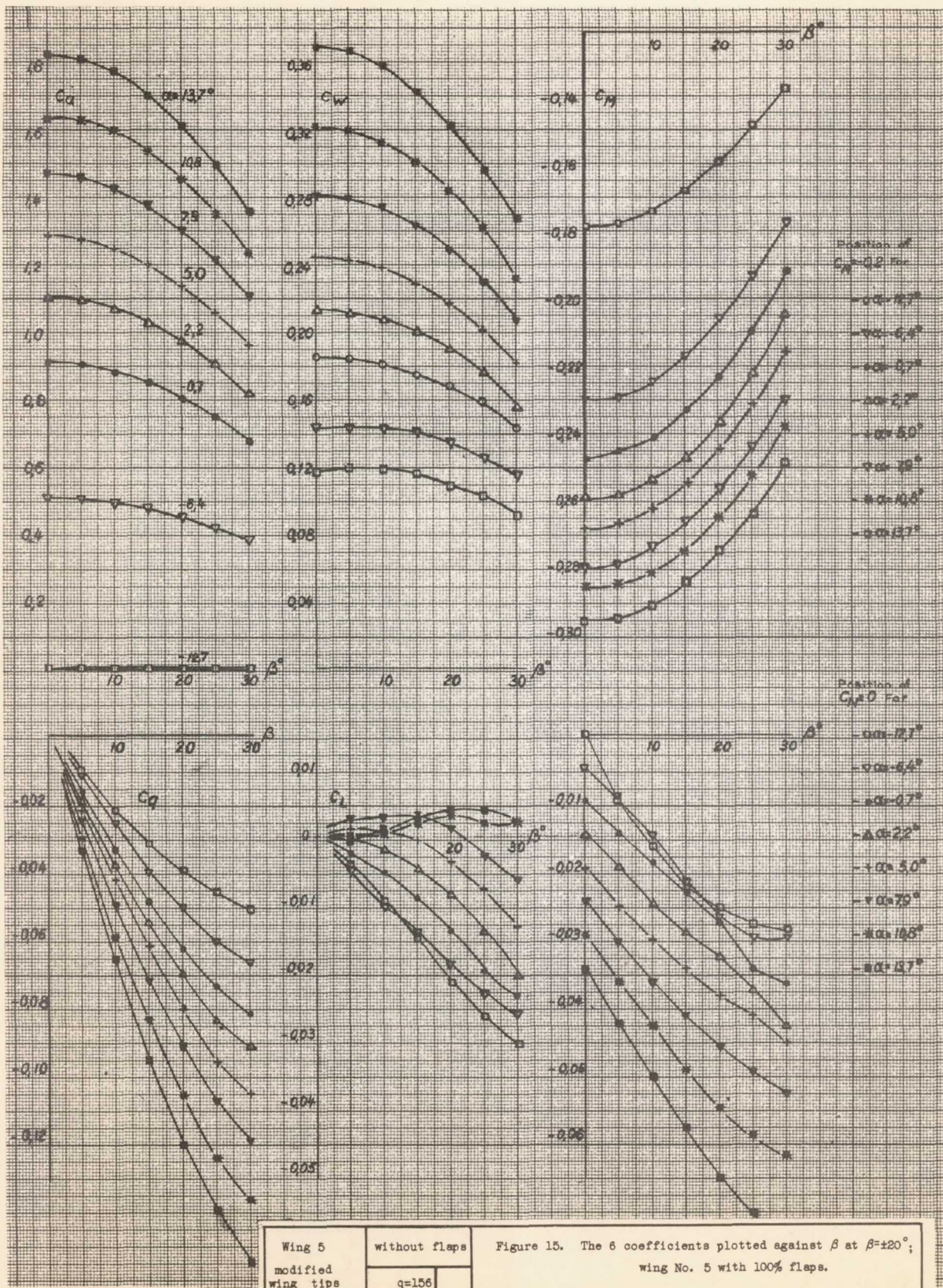
Figure 12. The 6 coefficients plotted against α at $\beta = \pm 20^\circ$; wing No. 5 with 100% flaps.

For $\beta = 20^\circ$ at c_q, c_L, c_N
the sign is to be inverted

Fig. 12







Wing 5 modified wing tips	without flaps	Figure 15. The 6 coefficients plotted against β at $\beta=20^\circ$; wing No. 5 with 100% flaps.
	q=156	

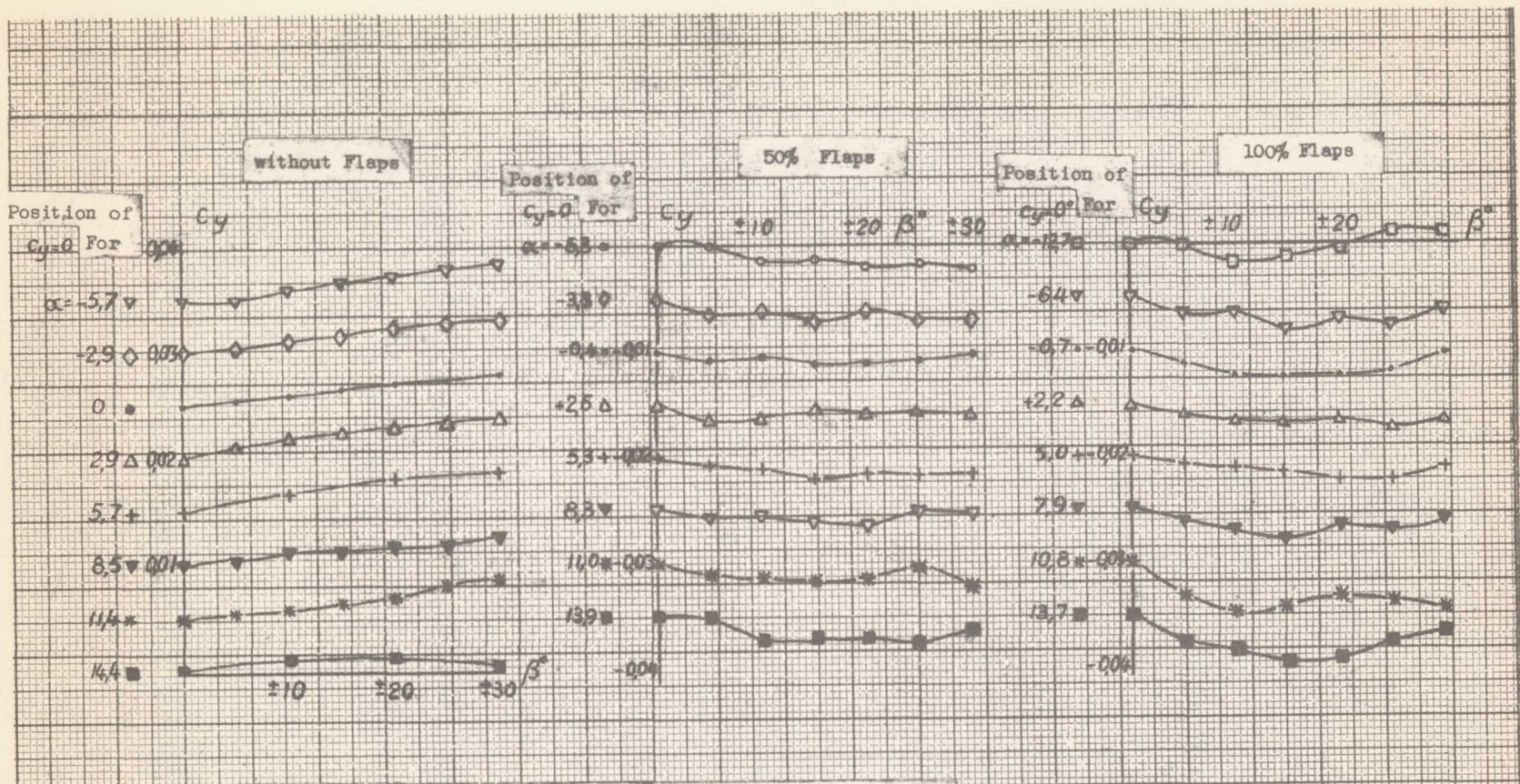
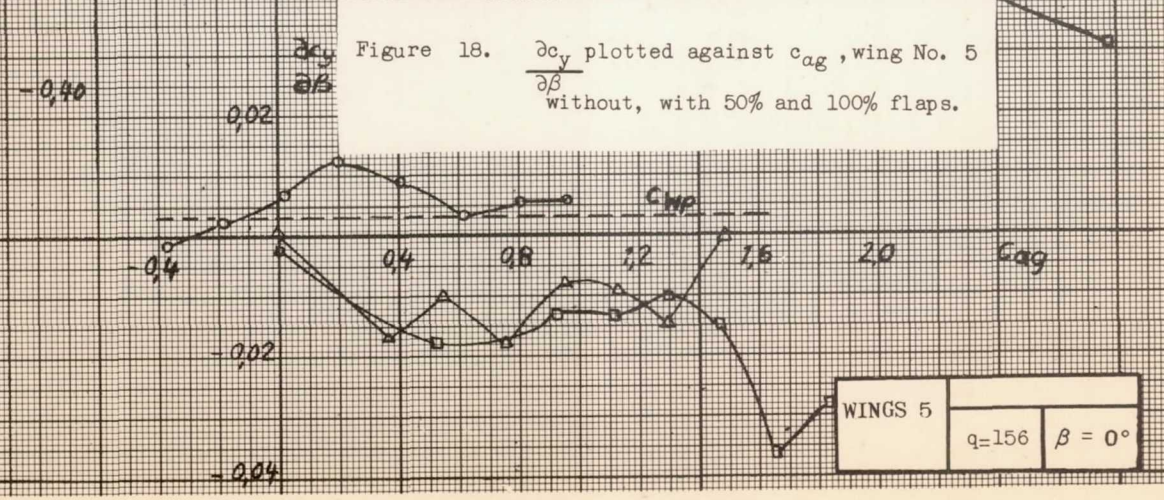
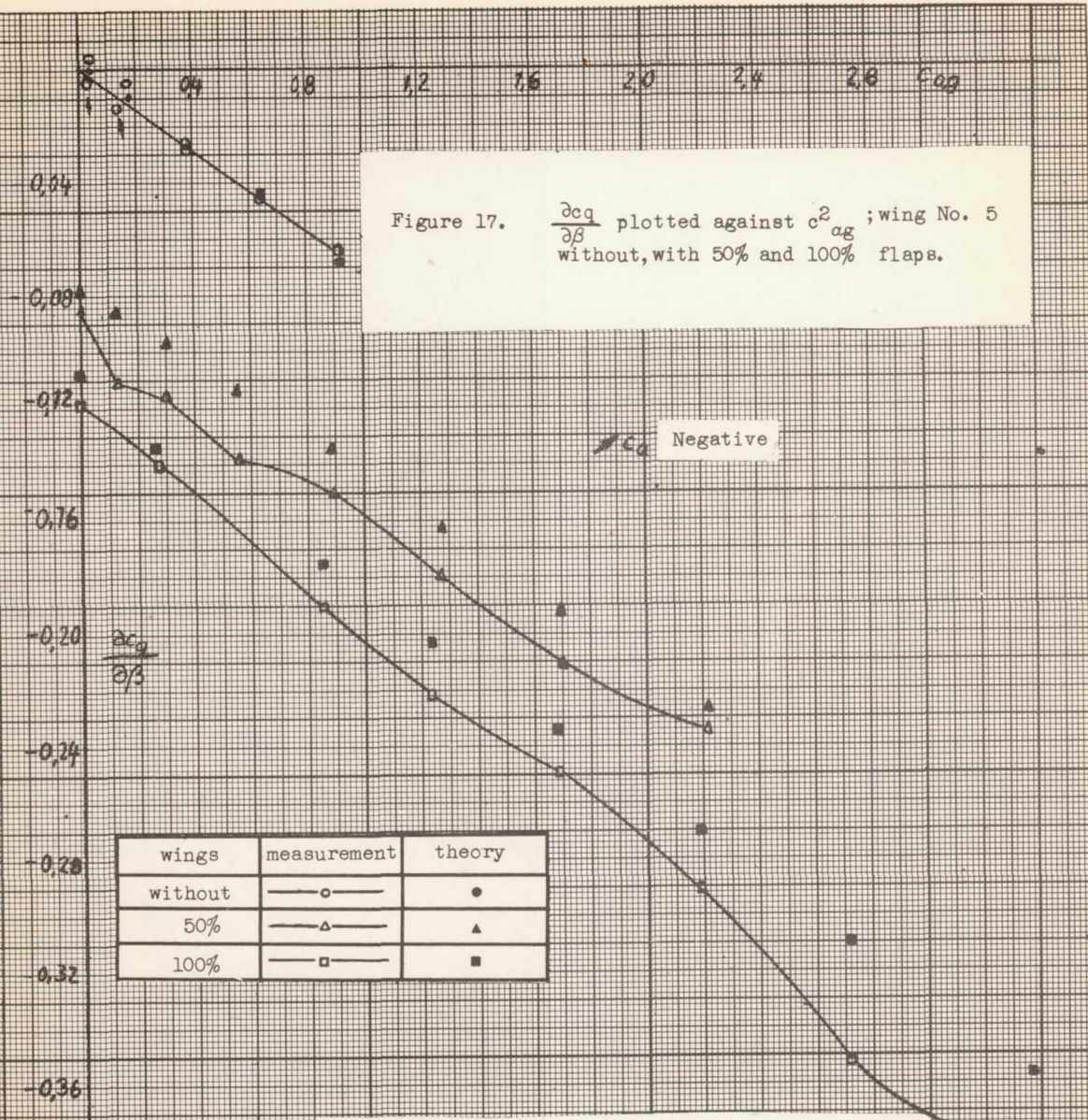


Figure 16. The coefficients of the cross-wind force plotted against β wing No. 5 without, with 50% and with 100% flaps.

WINGS 5	
q=156	



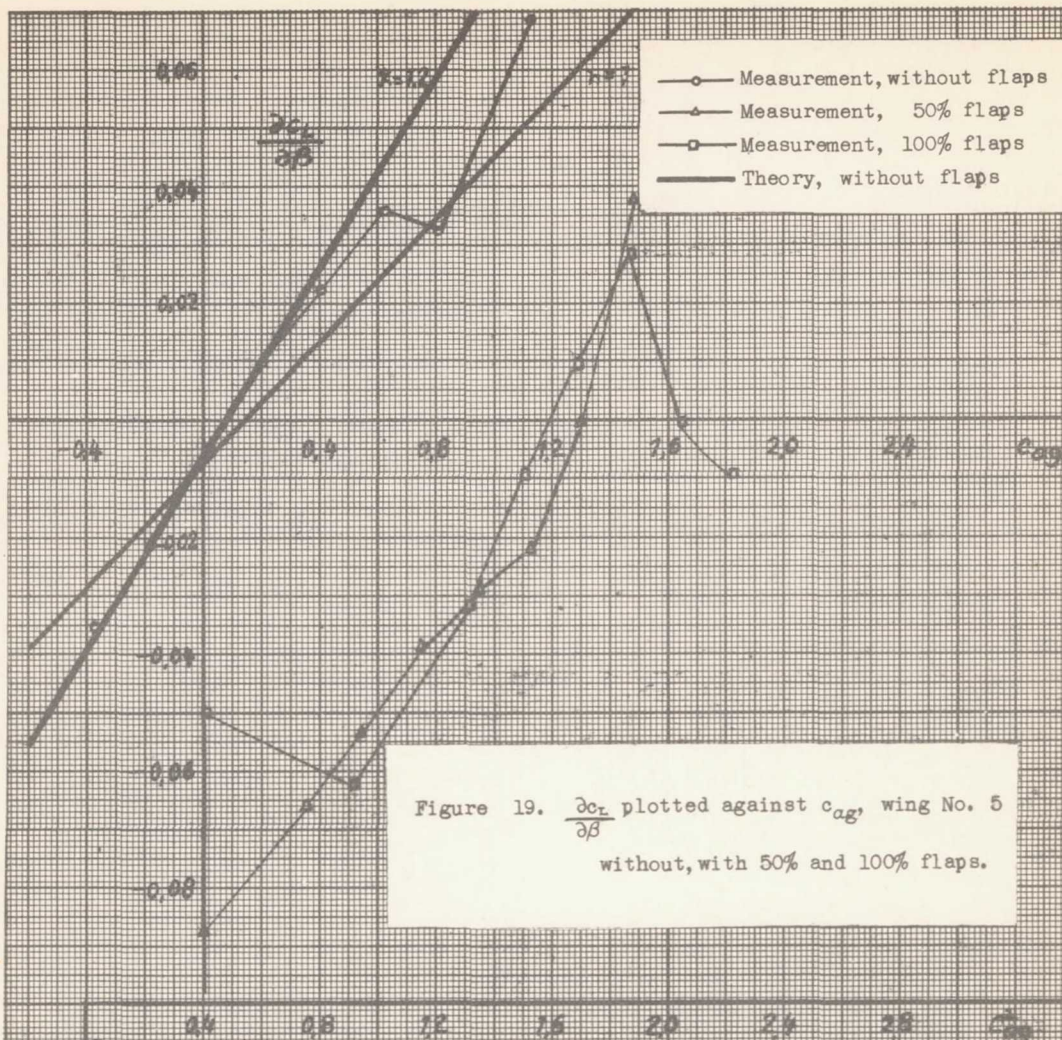


Figure 19. $\frac{\partial c_L}{\partial \beta}$ plotted against c_{ag} , wing No. 5 without, with 50% and 100% flaps.

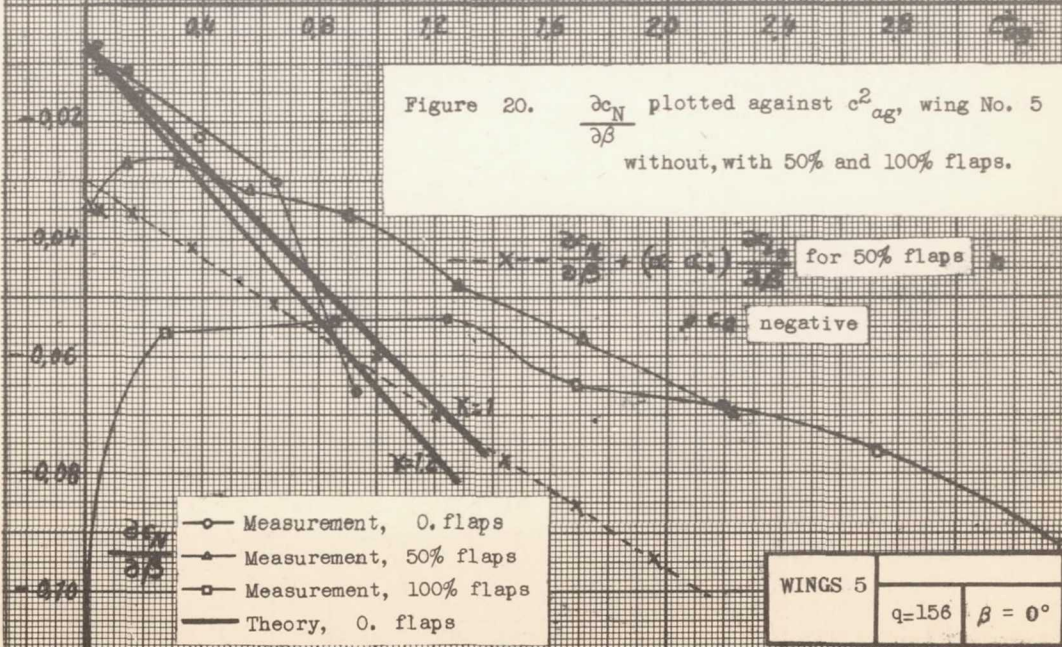
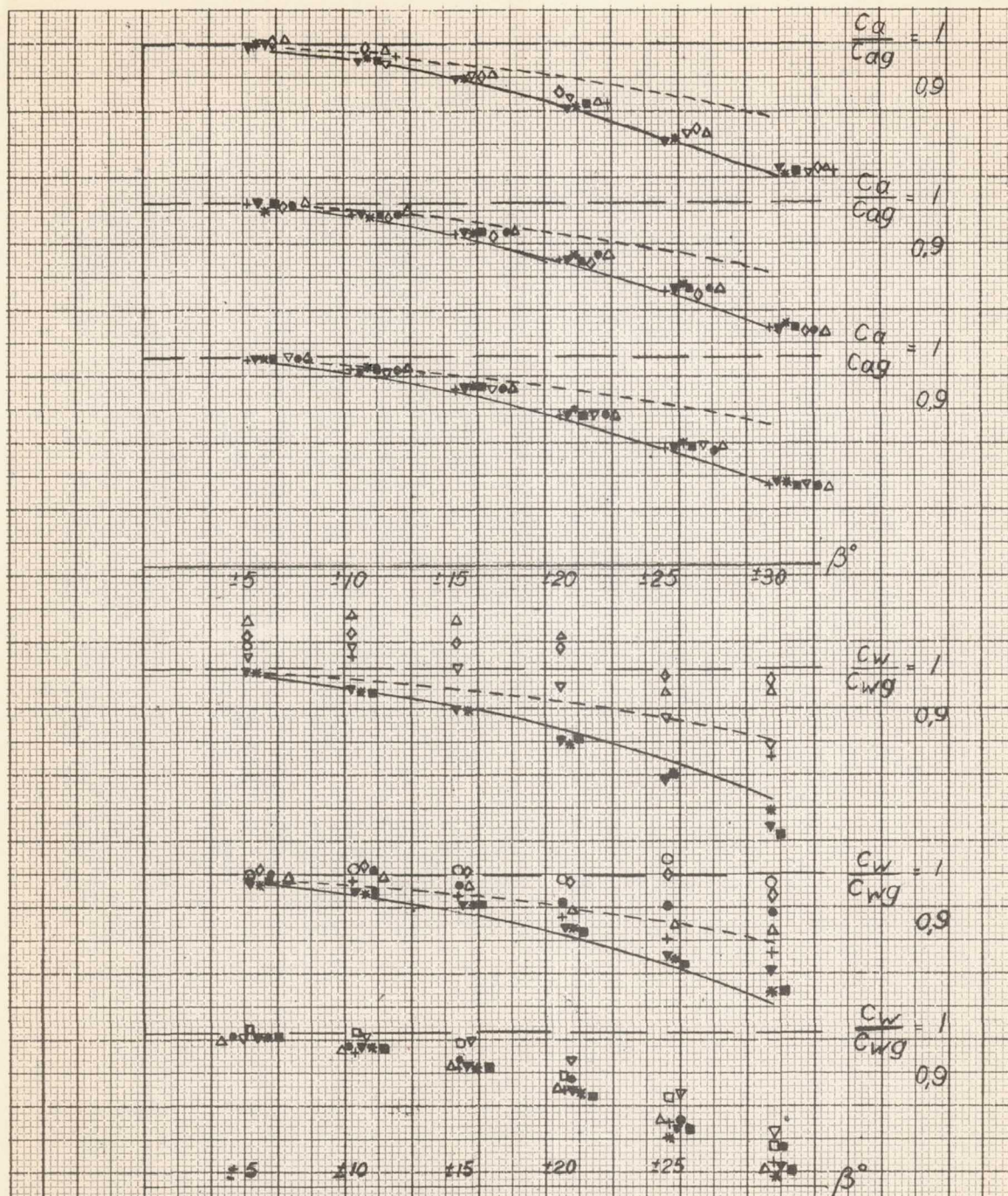


Figure 20. $\frac{\partial c_N}{\partial \beta}$ plotted against c_{ag}^2 , wing No. 5 without, with 50% and 100% flaps.

WINGS 5
 q=156 β = 0°

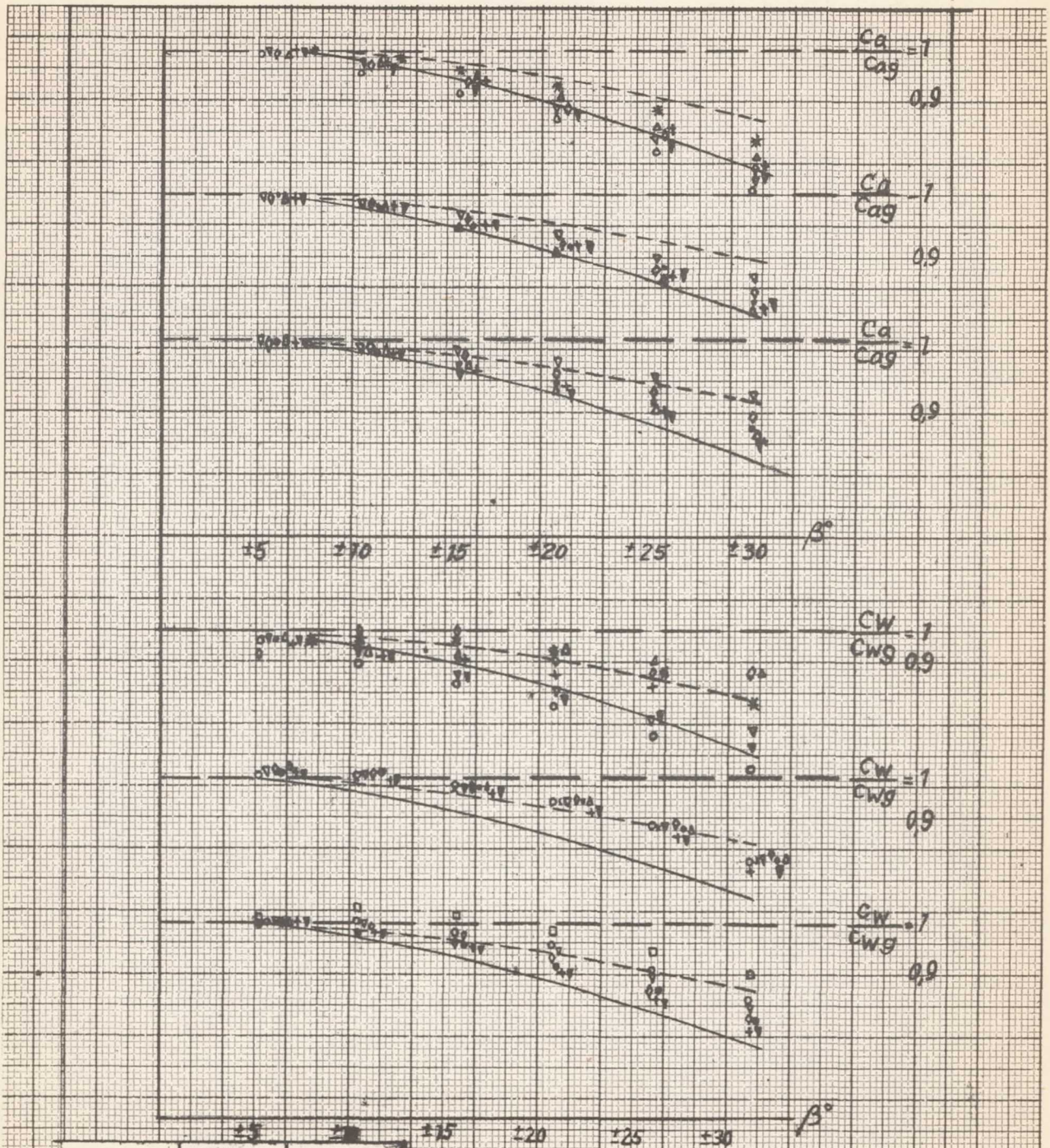


0. Flaps	50% Flaps	100% Flaps
▽ α = -5,7	◊ α = -8,3	□ α = -12,7
◊ α = -2,9	◊ α = -3,3	▽ α = -6,4
• α = -	• α = -0,4	• α = -0,7
△ α = 2,9	△ α = 2,5	△ α = 2,2
+ α = 5,7	+ α = 5,3	+ α = 5,0
▽ α = 8,5	▽ α = 8,3	▽ α = 7,9
* α = 11,4	* α = 11,0	* α = 10,6
■ α = 14,4	■ α = 13,9	■ α = 13,7

Figure 21. $\frac{c_a}{c_{ag}}$ and $\frac{c_w}{c_{wg}}$, plotted against β
 wing No. 5 without, with 50% and 100% flaps.

$\text{---} \frac{c_a}{c_{ag}}$
 $\text{---} \frac{c_w}{c_{wg}}$

WINGS 5		
	q=156	



0. Flaps	50% Flaps	100% Flaps
$\alpha = 8.7$	$\alpha = 8.8$	$\alpha = 7.0$
$\nu\alpha = 5.8$	$\nu\alpha = 8.0$	$\nu\alpha = 8.7$
$\delta\alpha = 2.9$	$\delta\alpha = 5.8$	$\delta\alpha = 6.0$
$\epsilon\alpha =$	$\epsilon\alpha = 2.9$	$\epsilon\alpha = 3.1$
$\Delta\alpha = 2.9$	$\Delta\alpha = 0$	$\Delta\alpha = 0.2$
$+\alpha = 5.8$	$\Delta\alpha = 2.9$	$\Delta\alpha = 2.7$
$\nu\alpha = 8.7$	$+\alpha = 5.8$	$+\alpha = 6.6$
$\nu\alpha = 12.0$	$\nu\alpha = 8.8$	$\nu\alpha = 8.5$

Figure 22. $\frac{c_a}{c_{ag}}$ and $\frac{c_w}{c_{wg}}$ plotted against β wing No. 9 without, with 50% and 100% flaps.

$\text{---} = \frac{c_a}{c_{ag}}$
 $\text{---} = \frac{c_w}{c_{wg}}$

WINGS 9	$q=156$
---------	---------

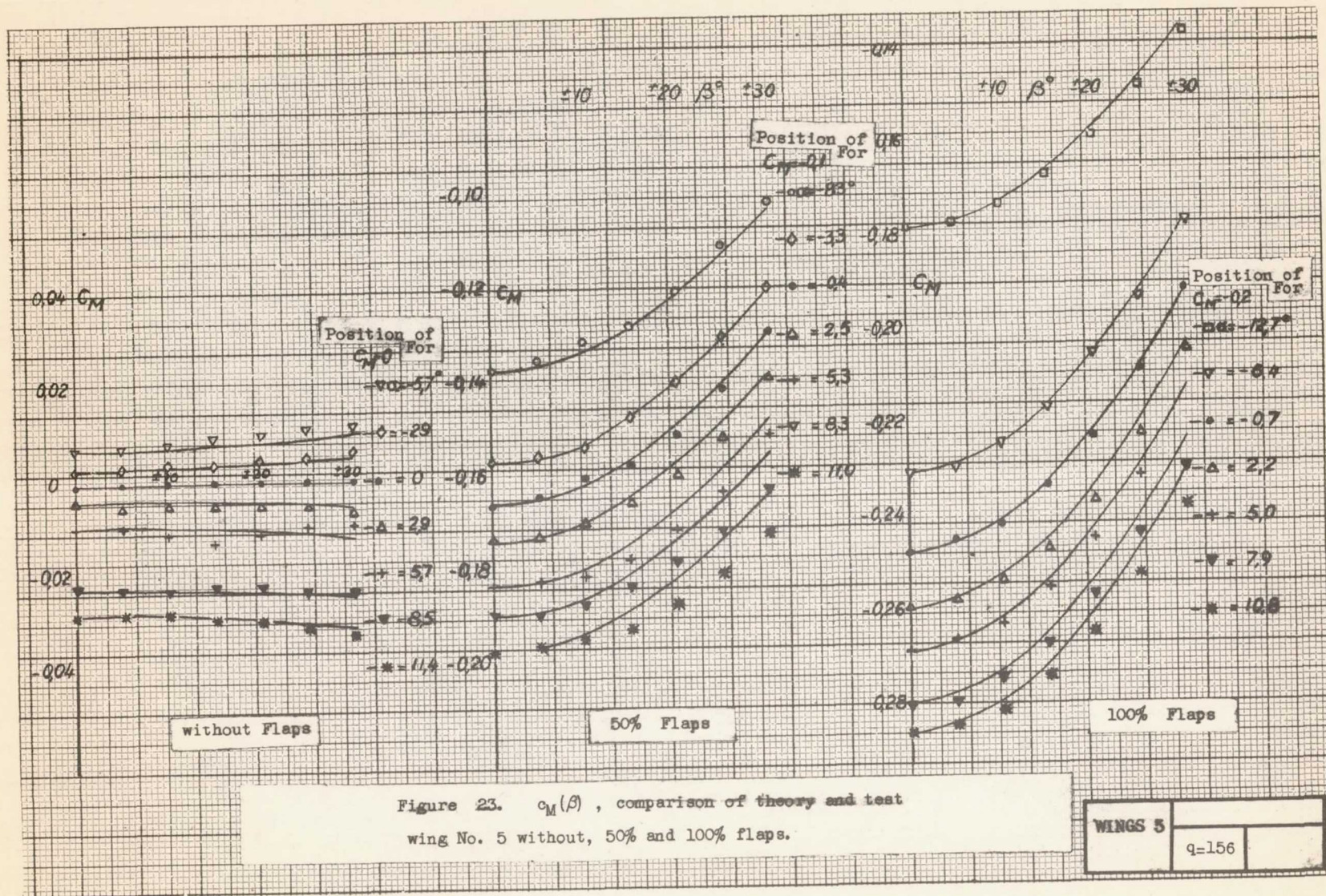


Figure 23. $C_M(\beta)$, comparison of theory and test wing No. 5 without, 50% and 100% flaps.

WINGS 5		
	q=156	

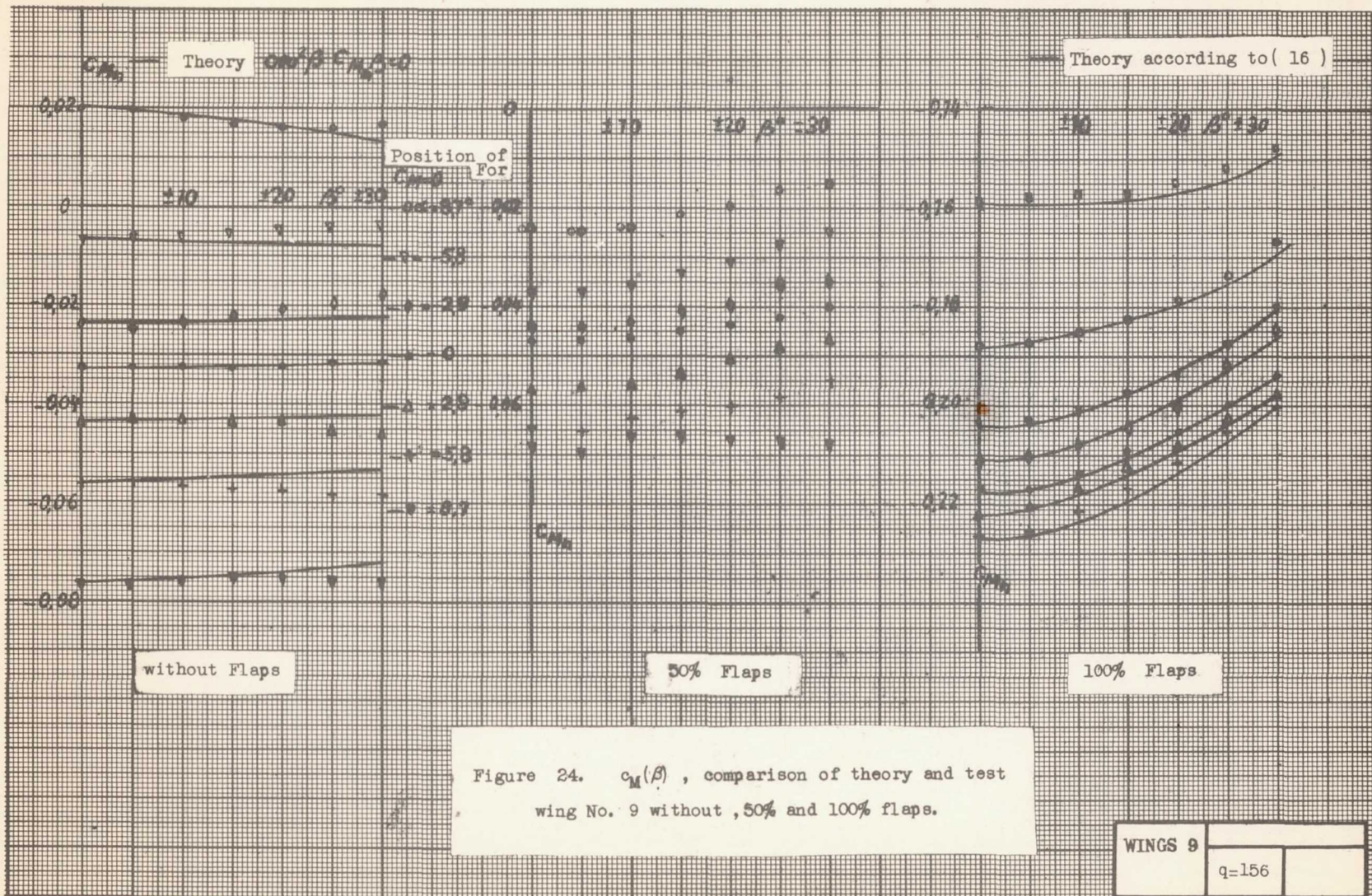


Figure 24. $c_m(\beta)$, comparison of theory and test wing No. 9 without, 50% and 100% flaps.

WINGS 9	
q=156	

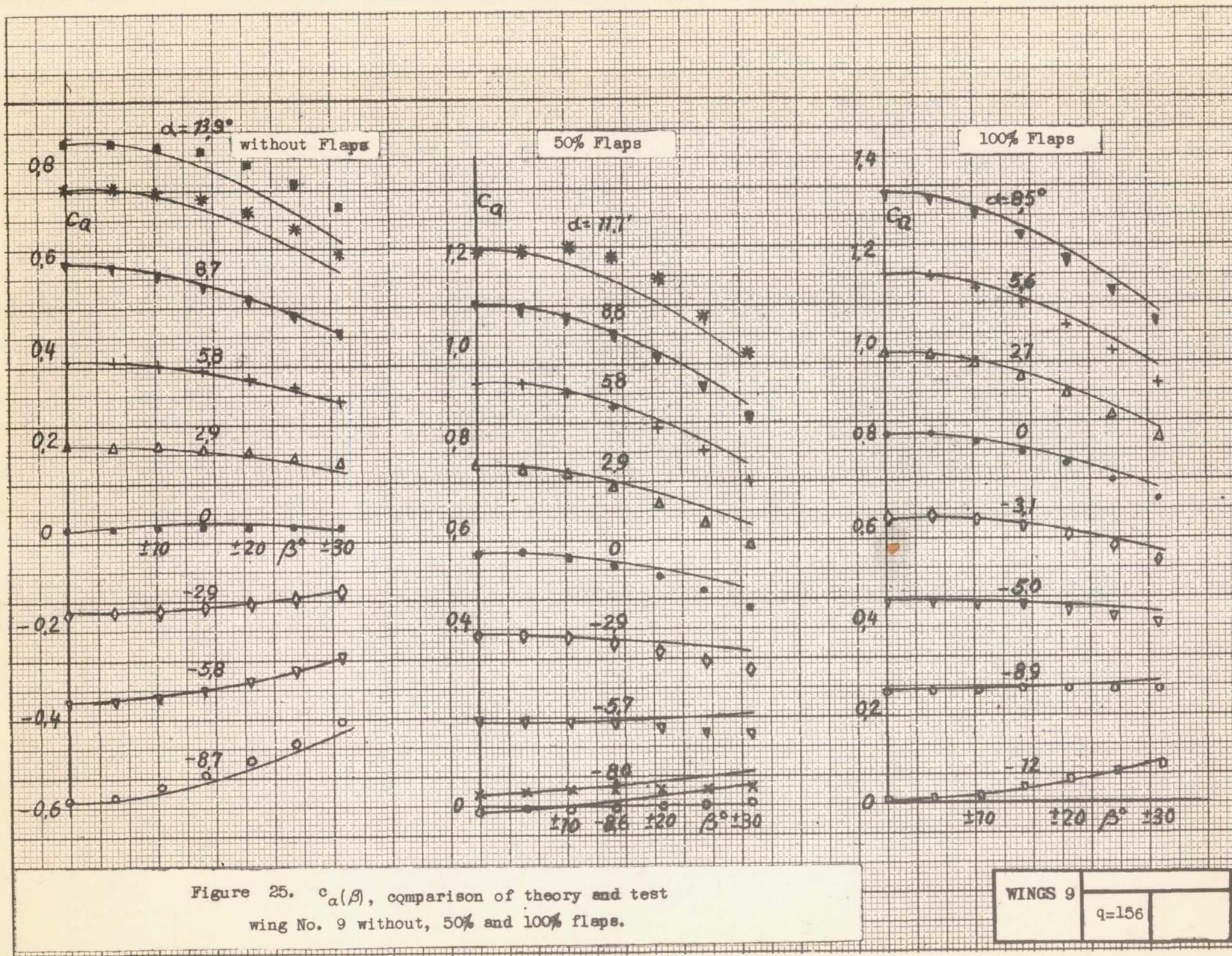
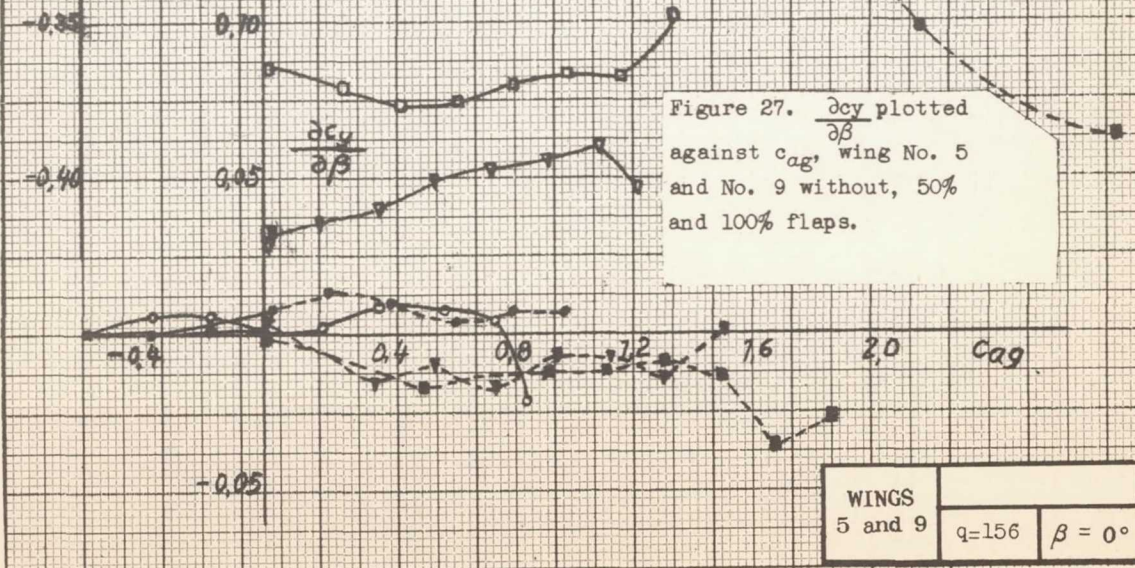
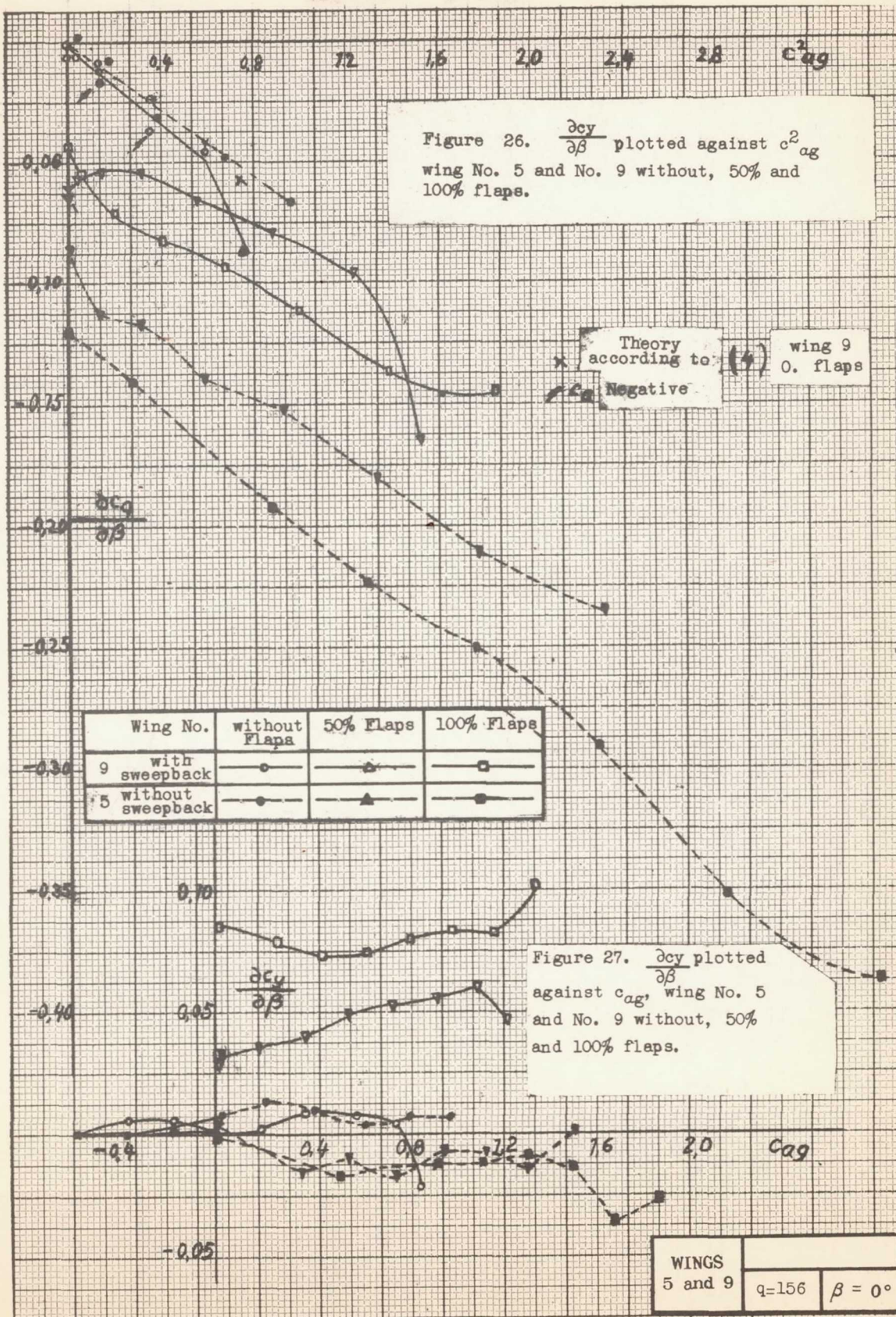


Figure 25. $C_a(\beta)$, comparison of theory and test wing No. 9 without, 50% and 100% flaps.

WINGS 9

q=156



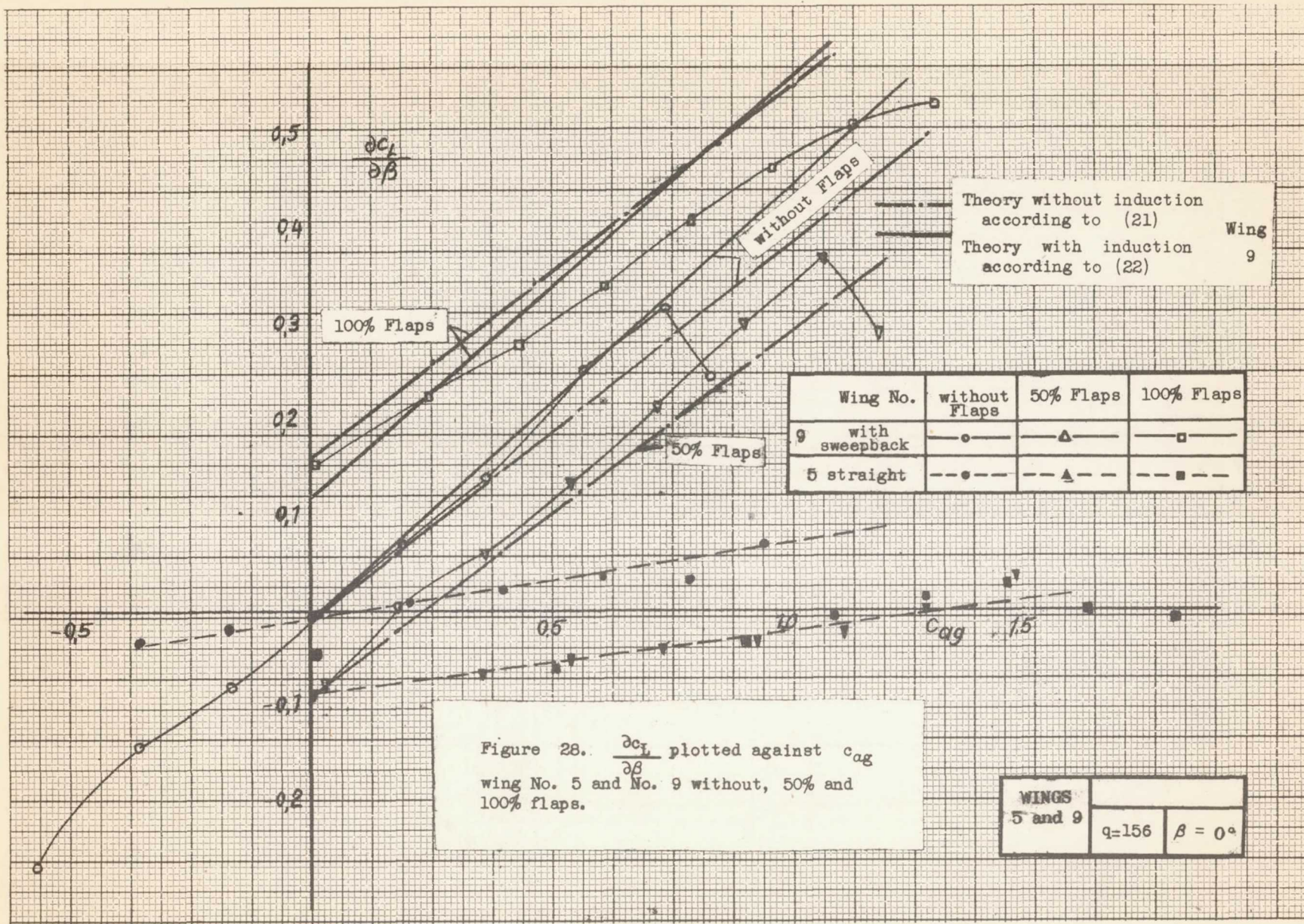
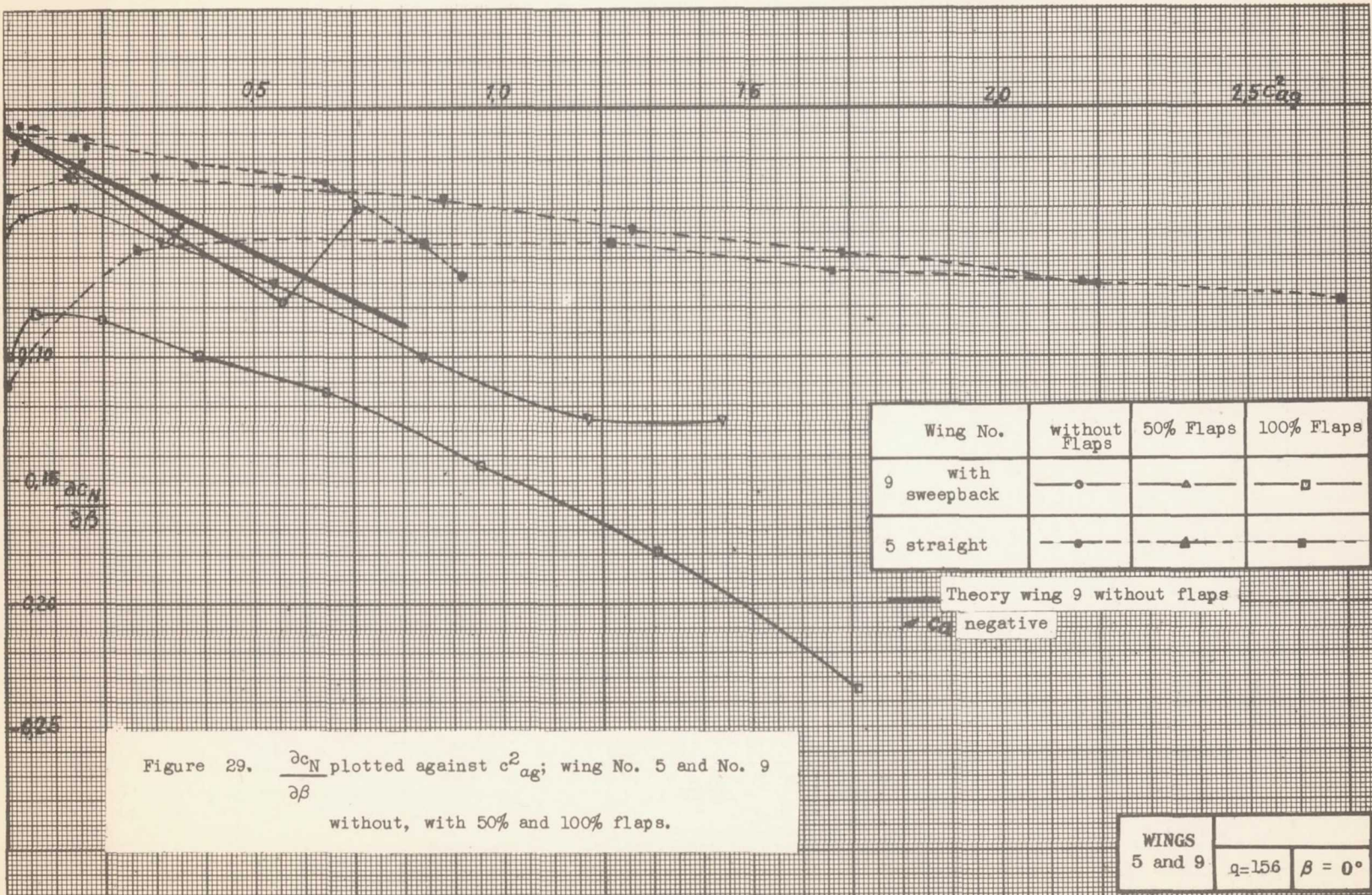


Figure 28. $\frac{\partial c_L}{\partial \beta}$ plotted against c_{ag} wing No. 5 and No. 9 without, 50% and 100% flaps.

WINGS 5 and 9		
	$q=156$	$\beta = 0^\circ$



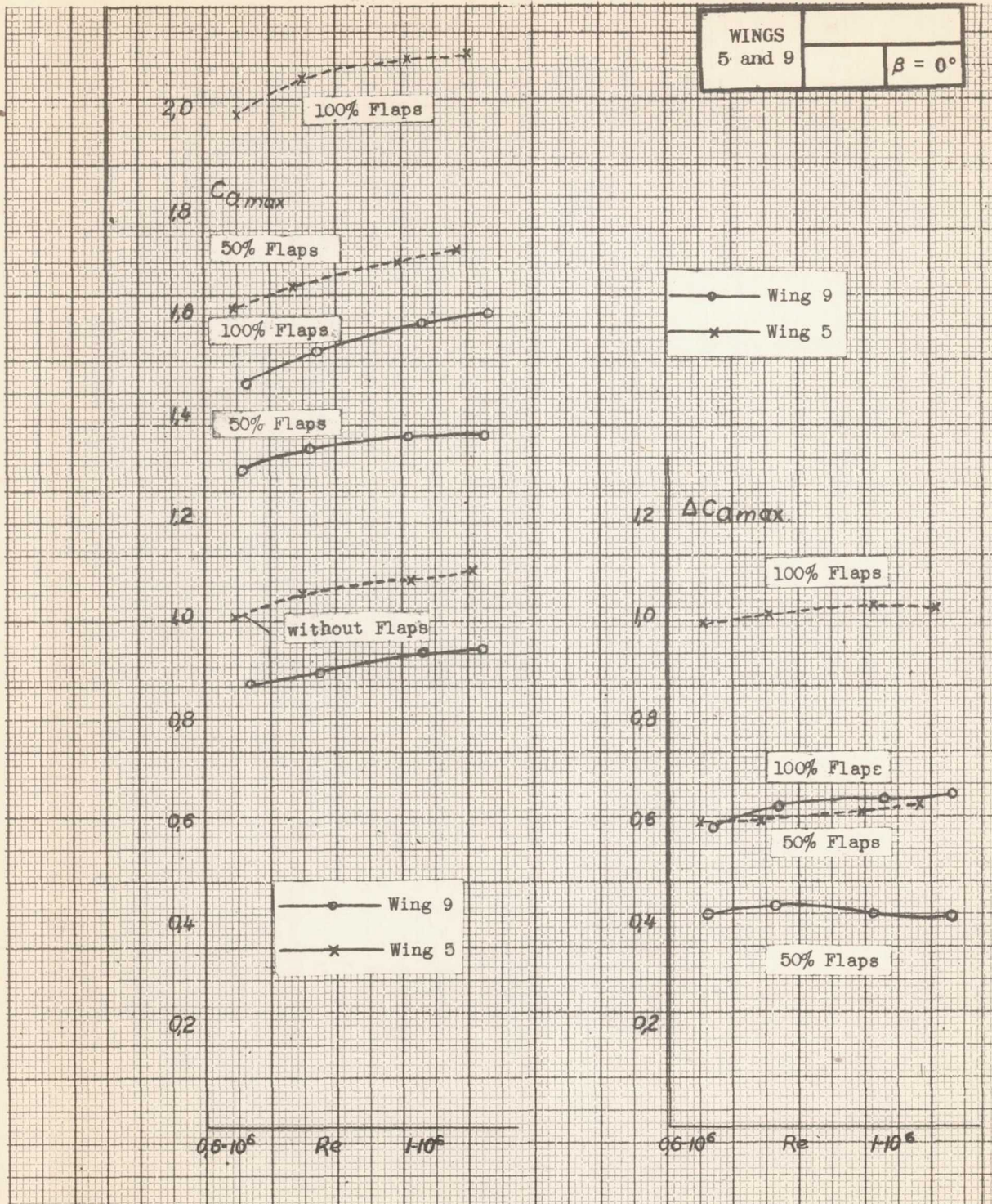


Figure 30. $c_{a\max}$ plotted against Re; wing No. 5 and 9 without, with 50% and 100% flaps.

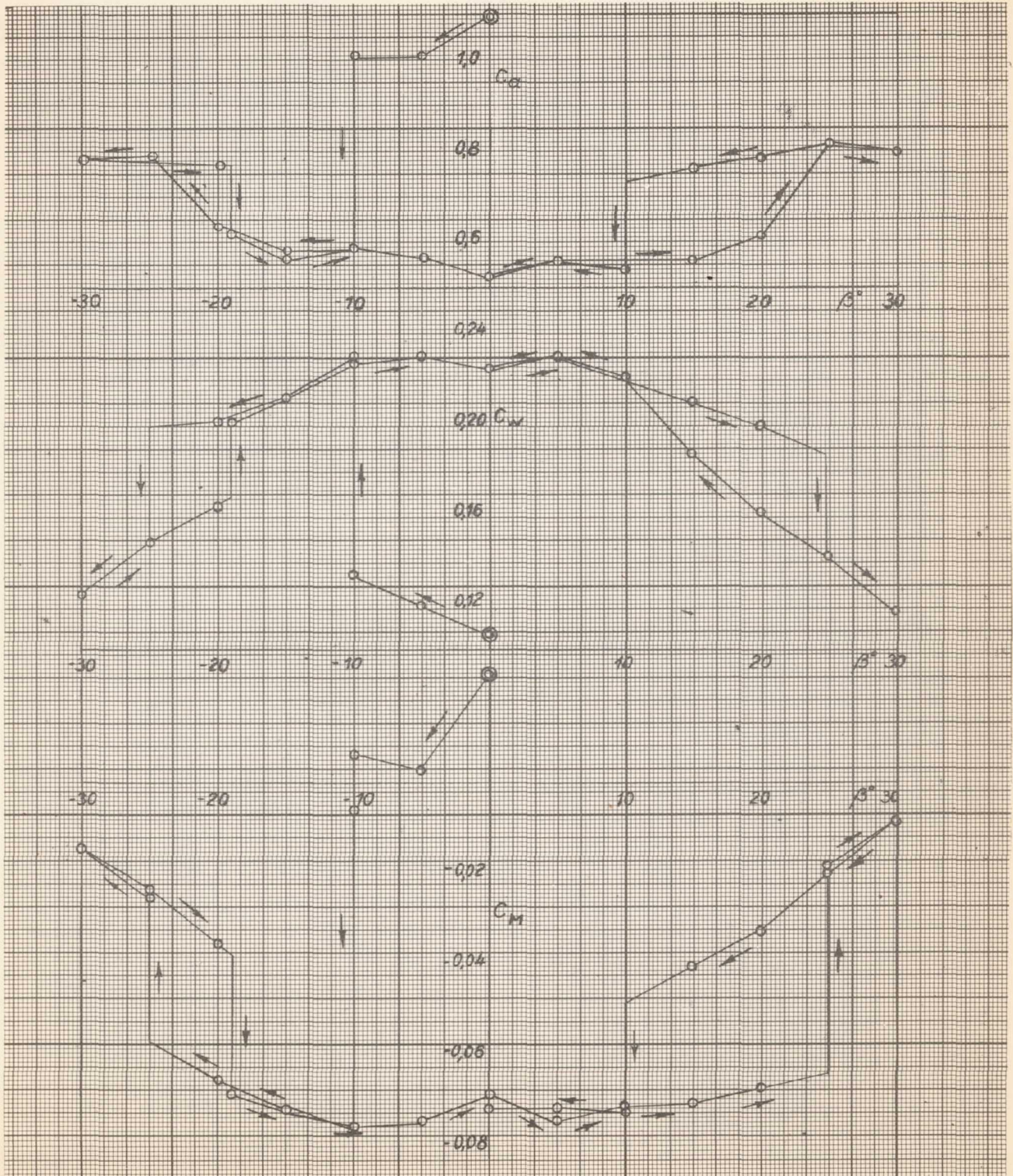
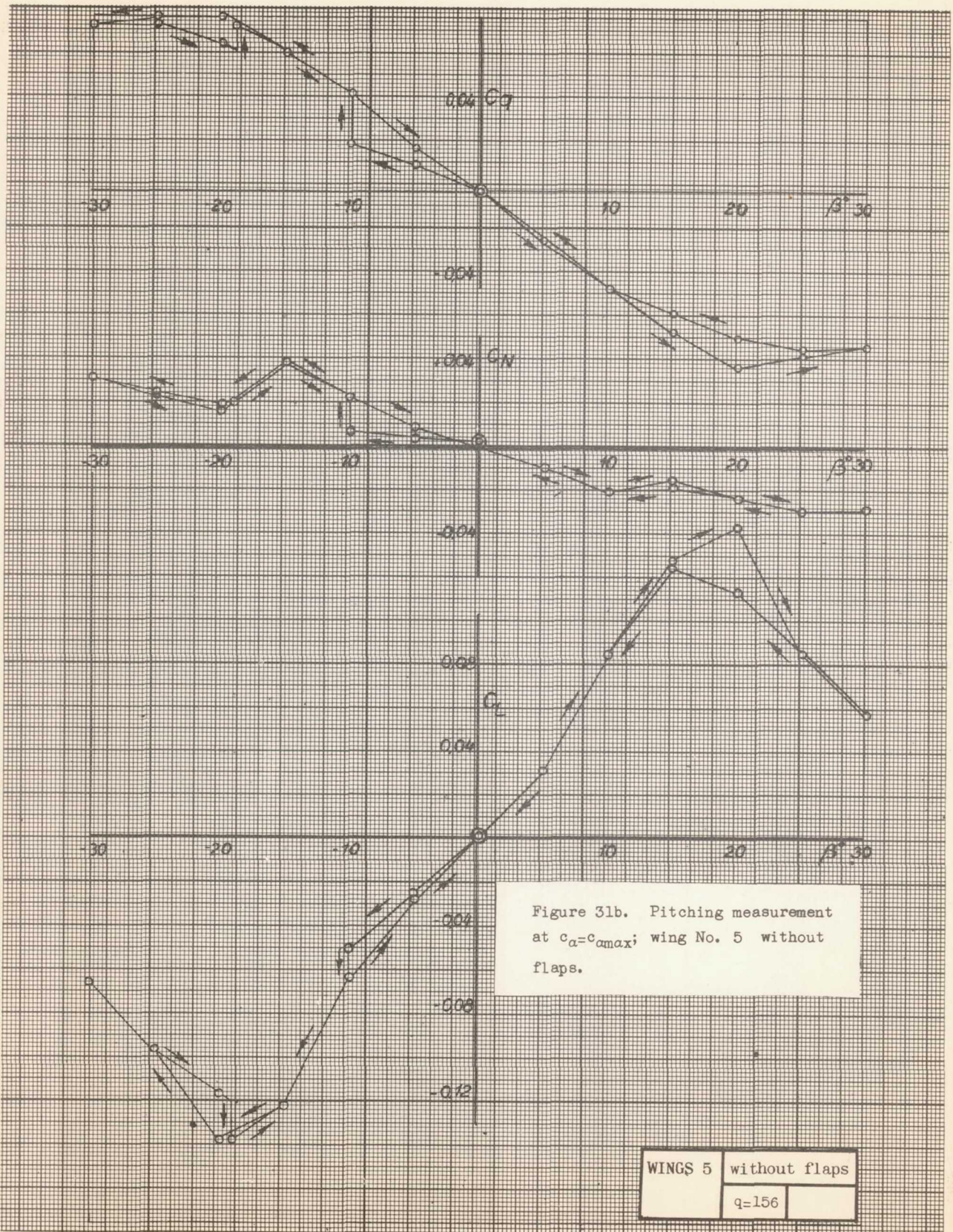


Figure 31a. Pitching measurement at $c_{\alpha}=c_{\alpha max}$; wing No. 5 without flaps.

WINGS 5	without flaps
	q=156



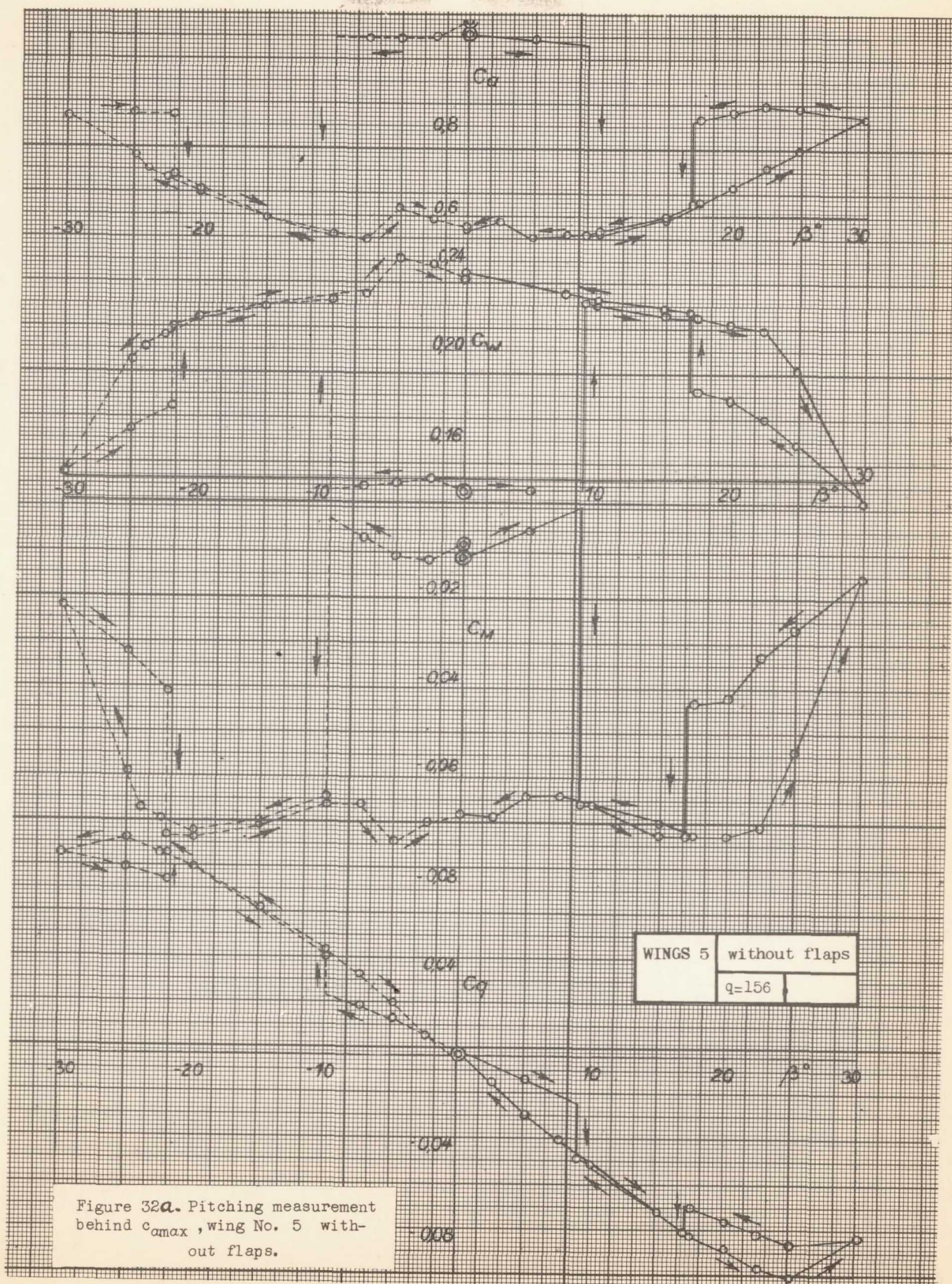


Figure 32a. Pitching measurement behind c_{amax} , wing No. 5 without flaps.

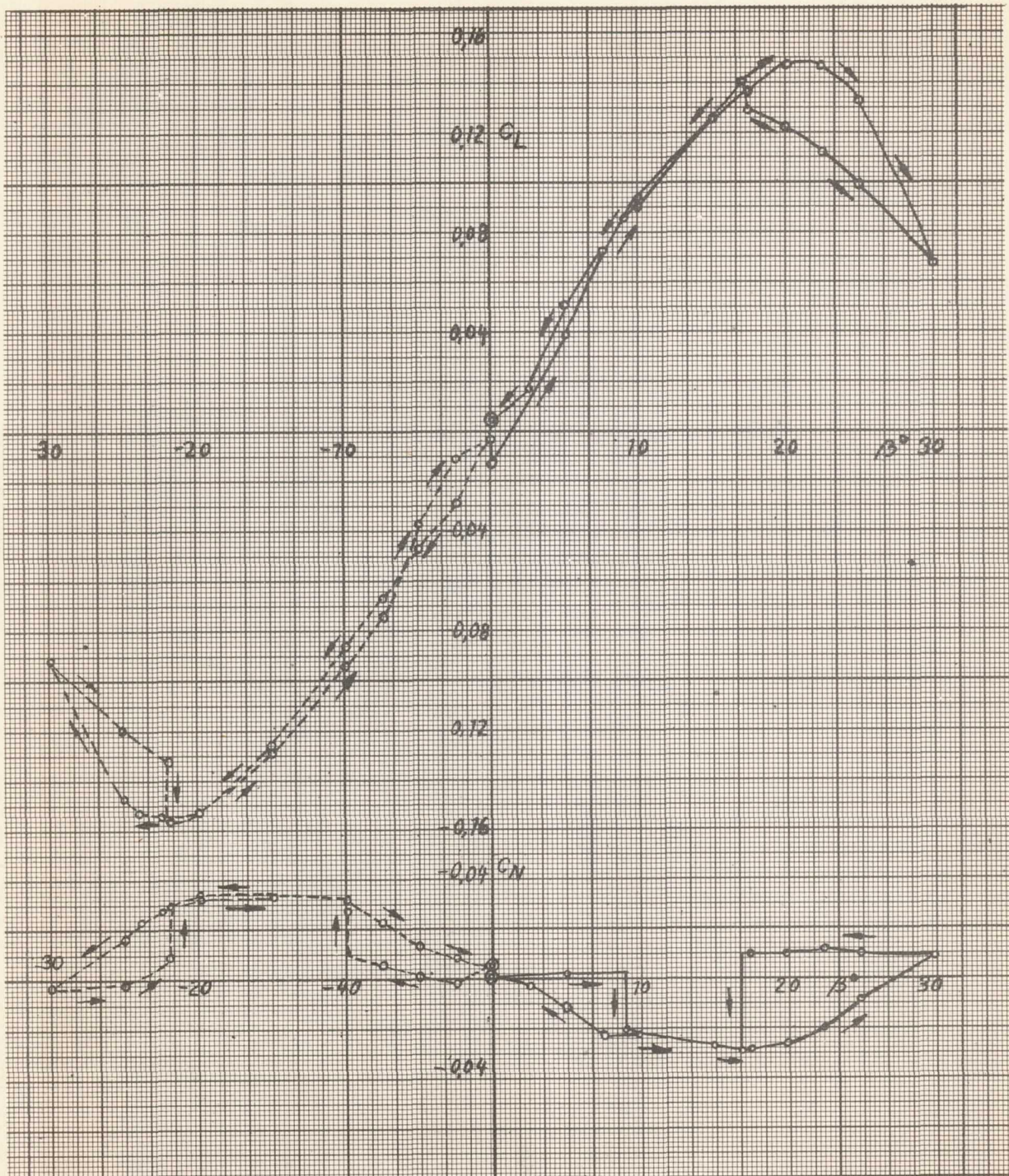
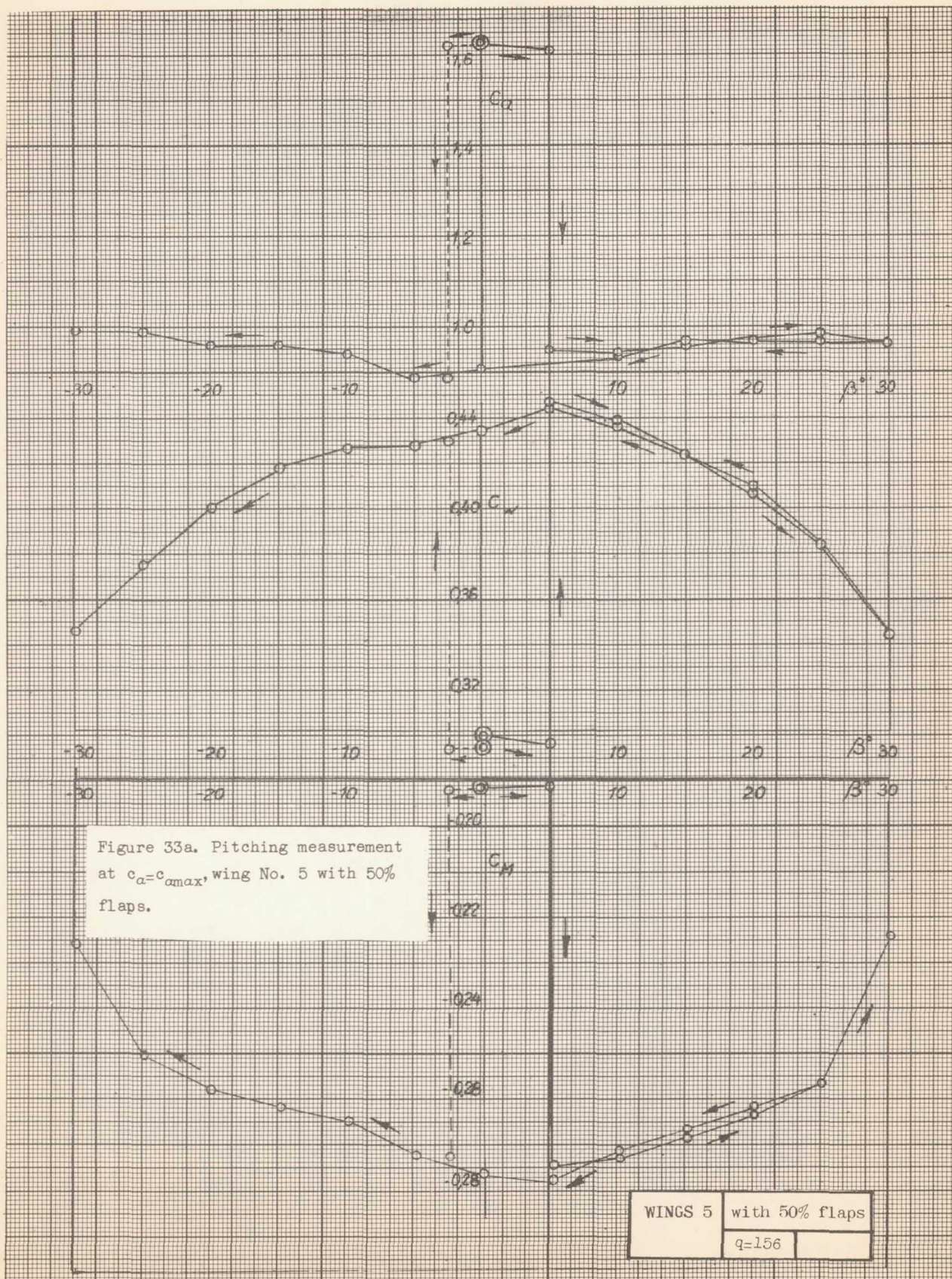
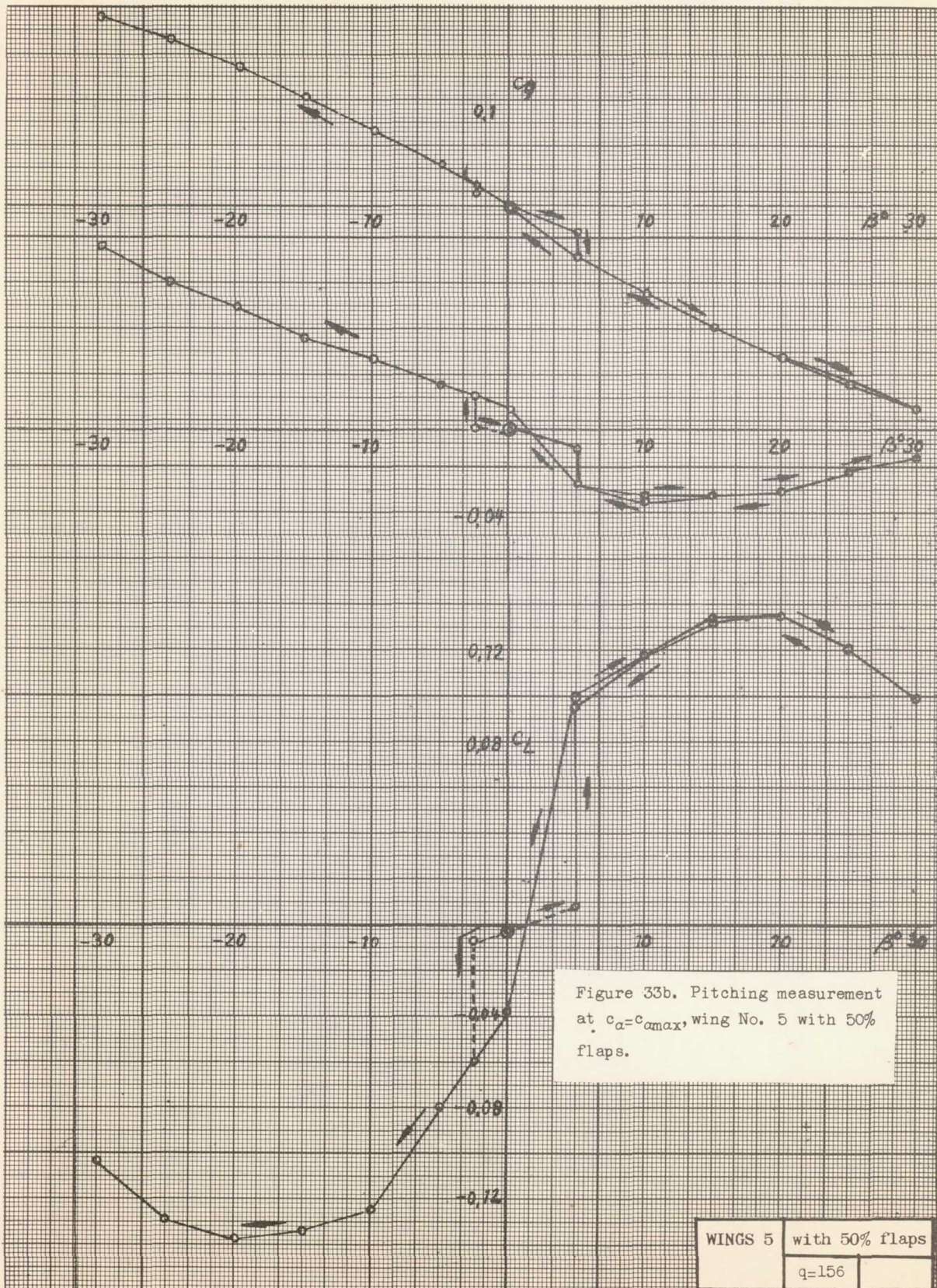
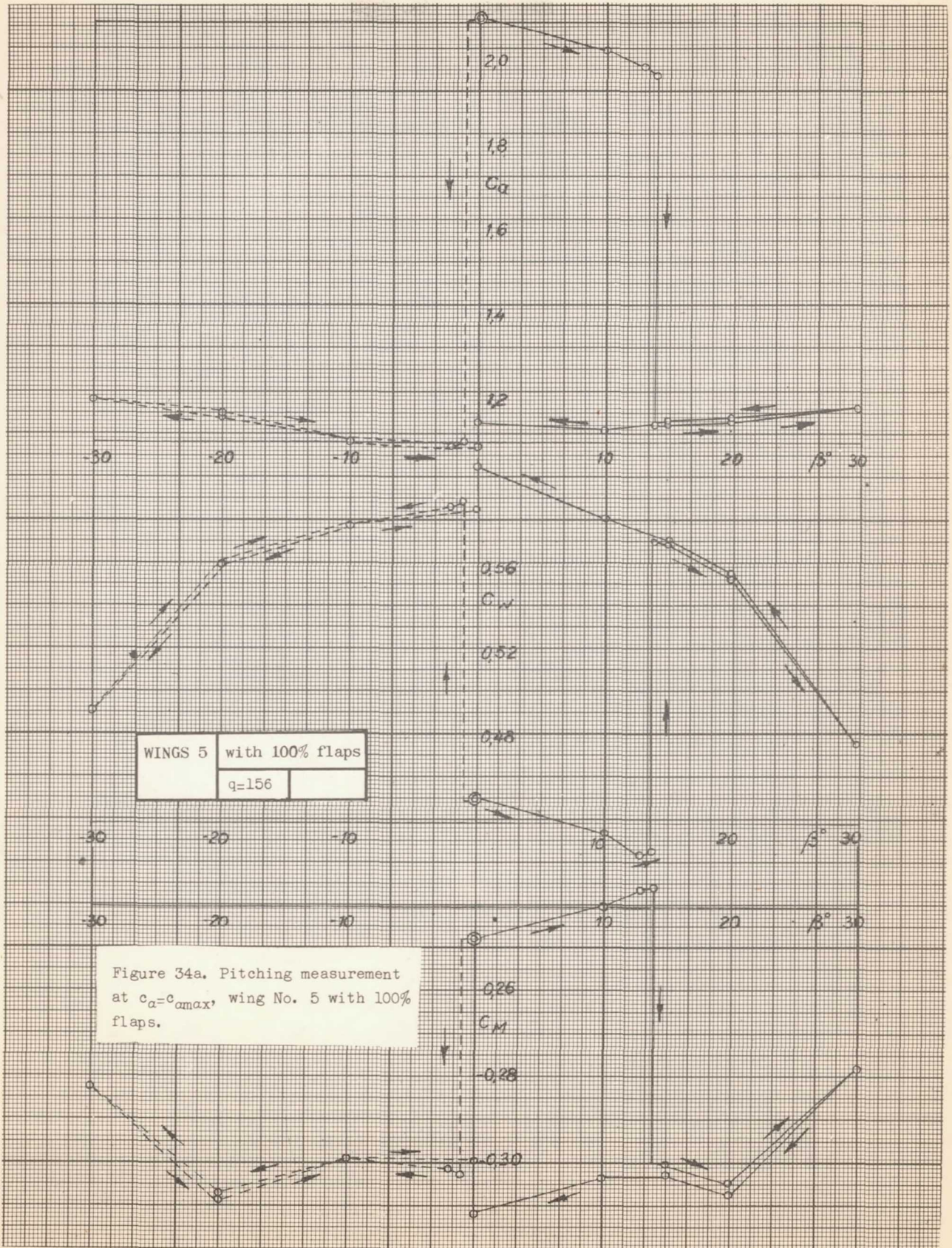


Figure 32b. Pitching measurement behind c_{amax} , wing No. 5 without flaps.

WINGS 5	without flaps
	q=156







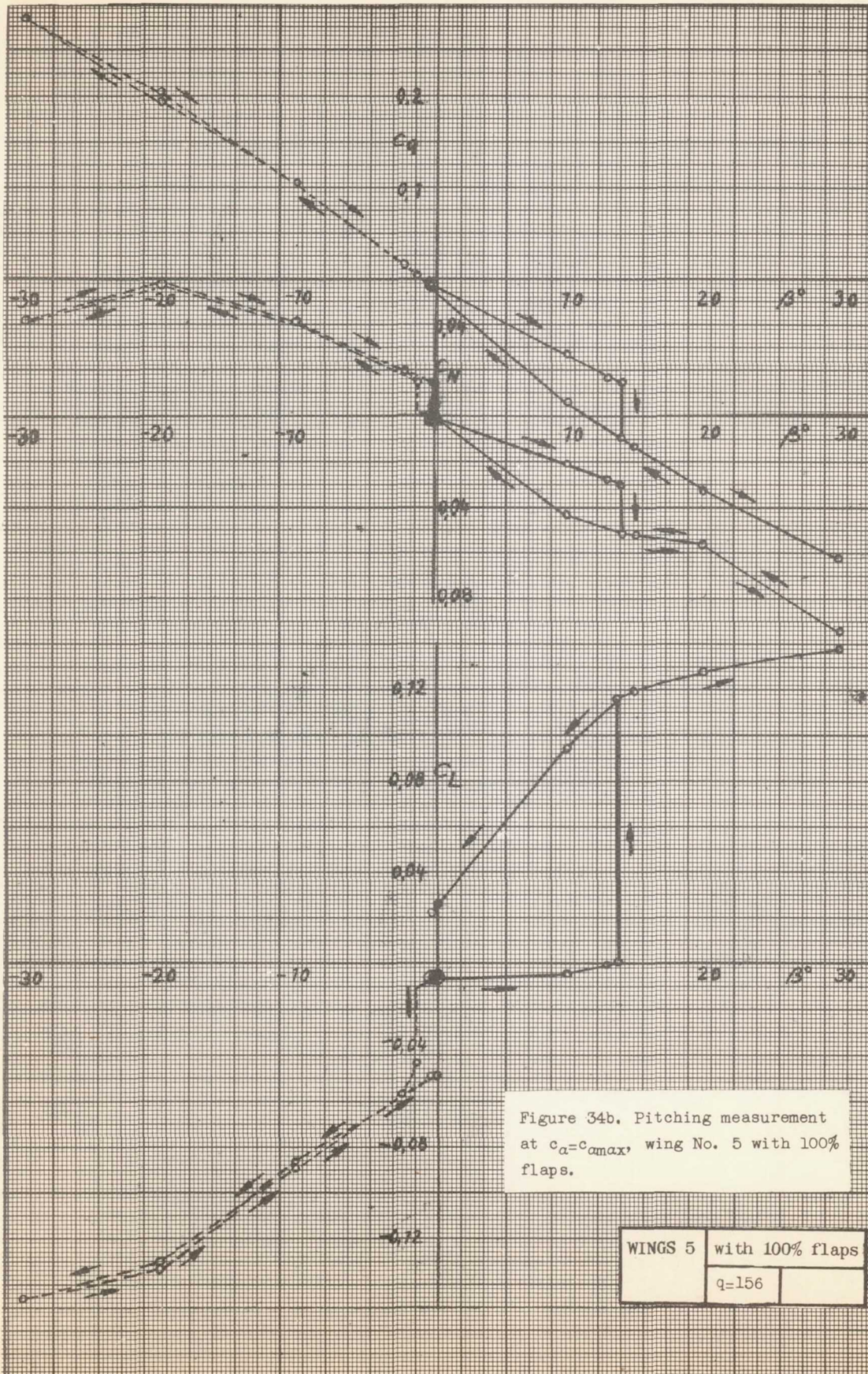


Figure 34b. Pitching measurement at $c_a=c_{amax}$, wing No. 5 with 100% flaps.

WINGS 5	with 100% flaps	
	q=156	